

**CFD SIMULATION OF TEMPERATURE DISTRIBUTION AND HEAT
TRANSFER PATTERN INSIDE C492 COMBUSTION FURNACE**

AMAR AL – FATHAH AHMAD

UNIVERSITI MALAYSIA PAHANG

UNIVERSITI MALAYSIA PAHANG

BORANG PENGESAHAN STATUS TESIS

JUDUL : CFD SIMULATION OF TEMPERATURE DISTRIBUTION AND
HEAT TRANSFER PATTERN INSIDE C492 COMBUSTION
FURNACE

SESI PENGAJIAN: 2008/2009

Saya AMAR AL – FATHAH BIN AHMAD
(HURUF BESAR)

mengaku membenarkan tesis Projek Sarjana Muda (PSM) ini disimpan di Perpustakaan Universiti Malaysia Pahang dengan syarat-syarat kegunaan seperti berikut:

1. Hakmilik kertas projek adalah di bawah nama penulis melainkan penulisan sebagai projek bersama dan dibiayai oleh UMP, hakmiliknya adalah kepunyaan UMP.
2. Naskah salinan di dalam bentuk kertas atau mikro hanya boleh dibuat dengan kebenaran bertulis daripada penulis.
3. Perpustakaan Universiti Malaysia Pahang dibenarkan membuat salinan untuk tujuan pengajian mereka.
4. Kertas projek hanya boleh diterbitkan dengan kebenaran penulis. Bayaran royalti adalah mengikut kadar yang dipersetujui kelak.
5. *Saya membenarkan/tidak membenarkan Perpustakaan membuat salinan kertas projek ni sebagai bahan pertukaran di antara institusi pengajian tinggi.
6. **Sila tandakan (✓)

☐

SULIT

(Mengandungi maklumat yang berdarjah keselamatan atau kepentingan Malaysia seperti yang termaktub di dalam AKTA RAHSIA RASMI 1972)

☐

TERHAD

(Mengandungi maklumat TERHAD yang telah ditentukan oleh organisasi/badan di mana penyelidikan dijalankan)

☒

TIDAK TERHAD

Disahkan oleh

(TANDATANGAN PENULIS)

Alamat Tetap: No 17, Jalan Perwira 1/12,
Taman Titiwangsa, 86000,
Kluang, Johor Darul Takzim

Tarikh: 21 April 2009

(TANDATANGAN PENYELIA)

ZULKAFI BIN HASSAN
Nama Penyelia

Tarikh: 21 April 2009

“I hereby declare that I have read this thesis and in my opinion this thesis has fulfilled the qualities and requirements for the award of Bachelor’s Degree of Chemical Engineering (Gas Technology)”.

Signature :
Supervisor’s Name : Prof. Madya Zulkafli Bin Hassan
Date : 21 APRIL 2009

**CFD SIMULATION OF TEMPERATURE DISTRIBUTION AND HEAT
TRANSFER PATTERN INSIDE C492 COMBUSTION FURNACE**

AMAR AL – FATHAH AHMAD

A thesis submitted in fulfilment for the award of the Degree of Bachelor in Chemical
Engineering (Gas Technology)

**Faculty of Chemical and Natural Resources Engineering
Universiti Malaysia Pahang**

APRIL 2009

I declare that this thesis entitled “CFD Simulation of Temperature Distribution and Heat Transfer Pattern inside C492 Combustion Furnace” is the result of my own research except as cited in the references. The thesis has not been accepted for any degree and is not concurrently submitted in candidature of any other degree.

Signature :

Name : Amar Al – Fathah Ahmad

Date : 21 APRIL 2009

*Dedicated, in thankful appreciation for support,
encouragement and understanding
to my beloved family and friends.*

ACNOWLEDGEMENT

In the name of Allah S.W.T. the most gracious and most merciful, Lord of the universe, with His permission Alhamdulillah the study has been completed. Praise to Prophet Muhammad S.A.W., His companions and to those on the path as what He preached upon, might Allah Almighty keep us His blessing and tenders.

First of all, I would like to express my gratitude to my research supervisor, Mr. Associate Professor Zulkafli Bin Hassan for his valuable guidance, advices, efforts, supervision and enthusiasm given throughout for the progress of this research. Although he always busy with his work, he can spend the time in completing this research.

I also wish to express my thankful to Mr. Mohd Masri A.Razak for conducting CFD class and gave so much guide and knowledge of the software. He has contributed towards my understanding and thoughts. Without the continued support and interest, this thesis would not have been the same as presented here.

I owe tremendous appreciation to my parents, Ahmad Md Isa and Siti Fatimah Ariffin for their support and motivation during the tough time throughout the duration of this study

Thank you so much for all. May Allah S.W.T. the Almighty be with us all the time.

ABSTRACT

Studies into the temperature distribution and heat transfer characteristics in a C492 combustion test furnace using commercial code FLUENT is presented in this paper. The mathematical model is based on an Eulerian description for the continuum phase and the model predicts gas flows, species concentrations and temperatures, particle trajectories and combustion and radiation heat fluxes. The gas phase conservation equations of momentum, enthalpy and mixture fraction are solved utilizing the k- ϵ turbulence model. Non premix combustion approach is used to predict the combustion process. The composition of the fuel component is setup using probability density function (PDF). A 3-D simplified model is created to determine the temperature and heat flux profiles and other thermal characteristics for a typical 150kW utility furnace firing liquid fuels or gaseous fuels. The temperature profiles of the furnace based on excess air ratio are predicted using the 3-D model. The main parameter is the excess air ratio consists of 1.248, 1.299, 1.362 and 1.417 which is used to study the temperature distribution. The model calculations showed a good agreement with the measured experimental data both in full and pilot scale of the test furnace as well as from the literature data. Using the experience gained from these CFD model studies can potentially improve the operation of a furnace, designing better combustion chamber or furnace with high performance and efficiency. Ultimately, these CFD model has the advantages of reduced cost, time and ability to optimize design significantly without much investment in the real experiment.

ABSTRAK

Kajian terhadap pengagihan suhu dan ciri – ciri pemindahan haba di dalam relau pembakaran C492 menggunakan kod FLUENT komersial dibentangkan di dalam kajian ini. Model matematik yang digunakan adalah berdasarkan Eulerian teori untuk fasa kontinuum dan digunakan untuk meramal pergerakan gas, kepekatan spesis dan suhu, trajektori partikel dan haba fluks pembakaran. Pemuliharaan persamaan momentum untuk fasa gas, entalpi, dan pecahan campuran diselesaikan menggunakan model pergolakan k- ϵ . “Non premix combustion” digunakan untuk meramal proses pembakaran di dalam simulasi ini. Komposisi bahan bakar ditetapkan menggunakan fungsi kebarangkalian ketumpatan (PDF). Model relau 3-D direka untuk menentukan suhu dan profil perbezaan haba serta lain – lain karakteristik thermal yang biasa untuk relau berkuasa 150kW yang menggunakan bahan api cecair atau gas. Profil - profil suhu bagi relau diramal berdasarkan kesan nisbah udara berlebihan ke atas model 3-D tersebut. Parameter utama digunakan adalah kesan nisbah udara berlebihan yang terdiri daripada 1.248, 1.299, 1.362 dan 1.417 dimana digunakan untuk mengkaji pengagihan suhu di dalam relau. Pengiraan model menunjukkan keputusan yang baik dimana menghampiri data – data dari eksperimen samada untuk relau di industri atau kajian kecil, malahan juga menghampiri data – data dari karya sastera. Pengalaman yang ditimba dari penggunaan kajian model CFD ini mampu meningkatkan operasi relau, mereka bentuk kebuk pembakaran atau relau yang lebih baik dan mempunyai kadar prestasi dan kecekapan yang tinggi. Akhirnya, model – model CFD ini mempunyai kelebihan dari segi pengurangan kos, masa dan kebolehan untuk memantapkan reka bentuk tanpa melibatkan eksperimen sebenar.

TABLE OF CONTENTS

CHAPTER	TITLE	PAGE
	ABSTRACT	v
	ABSTRAK	vi
	TABLE OF CONTENT	viii
	LIST OF TABLES	xi
	LIST OF FIGURES	xii
	LIST OF SYMBOLS	xiv
1	INTRODUCTION	
1.1	Research Background	1
1.1.1	Computational Fluid Dynamics	2
1.1.2	C492 Combustion Lab Unit	2
1.2	Problem Statement	3
1.3	Objectives	3
1.4	Scope of Study	4
1.5	Rationale and Significance	4

2**LITERATURE REVIEW**

2.1	Mathematical Modelling of NO _x Emission from High Temperature Air with Nitrous Oxide Mechanism	5
2.1.1	Effects of NO Model on the NO Formations	7
2.2	Summary of Previous Studies	9
2.3	Combustion Theory	9
2.3.1	Combustion Efficiency	11
2.4	Air Fuel Ratio	12
2.4.1	Effect of Excess Air Ratio	12
2.5	Liquefied Petroleum Gas (LPG)	13
2.6	Background of Study	14
2.6.1	Computational Fluid Dynamics (CFD)	14
2.6.1.1	Definition of CFD	14
2.6.1.2	History of CFD	15
2.6.1.3	Advantages of CFD	16
2.6.2	C492 Combustion Lab Unit	17
2.6.2.1	C492 Combustion Lab Unit Configuration	19

3**RESEARCH METHODOLOGY**

3.1	Overall Methodology	21
3.2	CFD Modelling and Simulation	22
3.3	Problem Solving Steps	23
3.3.1	Geometry Design/Meshing Geometry - GAMBIT	24

3.3.1.1	The Combustion Chamber Geometry and Materials	25
3.3.1.2	Combustion Chamber Meshing	25
3.3.2	FLUENT Simulation	27
3.3.2.1	CFD Computational Tools	27
3.3.2.2	CFD Governing Equations	28
3.3.2.2.1	Conservation Equations	28
3.3.2.3	Turbulence Modelling	29
3.3.2.4	FLUENT Discretisation	29
3.4	Experimental Methodology	31
3.4.1	Experimental Methodology Outline	32
3.4.2	Materials and Equipments	33
3.4.3	Operating Procedure	33
3.4.4	Experimental Procedure	34
4	RESULTS AND DISCUSSIONS	
4.1	Introduction	35
4.2	Experimental Results	36
4.3	Simulation Results	37
4.3.1	Temperature Distribution at Side View of Geometry	37
4.4	Comparison Between Simulation and Experimental Results	39
5	CONCLUSION AND RECCOMENDATIONS	
5.1	Conclusion	42
5.2	Recommendations	43

REFERENCES	44
APPENDIX A: CFD COMPUTATIONAL TOOLS	47
APPENDIX B: FUEL PROPERTIES	64
APPENDIX C: FLUENT SIMULATION RESULTS	69
APPENDIX D: EXPERIMENTAL DATA	81

LIST OF TABLES

TABLE NO.	TITLE	PAGE
2.1	Summary of Literature Review	9
3.1	Boundary Conditions	30
4.1	Experimental Results	36
4.2	Comparison of Flue Temperature	40
4.3	Comparison of Flame Temperature	40

LIST OF FIGURES

FIGURE NO.	TITLE	PAGE
2.1	Effects of excess air ratio on NO emission	6
2.2	Effect of excess air ratio on maximum temperature	7
2.3	Temperature distribution at the cross section through fuel and one air nozzle in the test furnace at different excess air ratio (λ)	8
2.4	C492 Combustion Lab Unit	18
2.5	Control Panel of C492 Combustion Lab Unit	18
2.6	Schematic Diagram of Gas Burner fitted on C493 Combustion Lab Unit	19
3.1	Flow charts of research methodology	22
3.2	Program Structure	23
3.3	Steps of CFD analysis	24
3.4	Overall combustion chamber dimension	25
3.5	Meshed combustion chamber geometry	26

3.6	Iteration process	31
3.7	Flow chart of experimental methodology	33
4.1	Temperature distribution at cross section through fuel and air nozzle in furnace at different excess air ratio (λ) at level 20 distribution	38
4.2	Flame cross section through fuel and air nozzle in furnace at different excess air ratio (λ) at level 3 distribution	38
4.3	Velocity vector based on total temperature of the furnace.	39
4.4	Effect of excess air ratio on flue temperature and flame temperature	41

LIST OF SYMBOLS

LPG	-	Liquefied Petroleum Gas
CFD	-	Computational Fluid Dynamics
CAD	-	Computer aided design
CAE	-	Computer aided engineering
RANS	-	Reynolds averaged Navier Stokes
OD	-	Outside diameter
ID	-	Inside diameter
CO ₂	-	Carbon dioxide
NO _x	-	Oxides of Nitrogen
AFR	-	Air fuel ratio
O ₂	-	Oxygen
kW	-	Kilowatts
K	-	Kelvin
CH ₄	-	Methane
C ₂ H ₆	-	Ethane
C ₃ H ₈	-	Propane
C ₄ H ₁₀	-	Butane
F	-	Force
m	-	mass
a		acceleration

PIC	Particle in cell
MAC	Marker and Cell
ALE	Arbitrary Lagrangian Eulerian
PDF	Probability density function
mm	millimetre
kg	kilogram
V	volt
n_c	Combustion efficiency
λ	Excess air ratio

CHAPTER 1

INTRODUCTION

1.1 Research Background

Space heating is very important in industrial sector. It emphasis on effective heat transfer, and heat is supplied through furnace, burner or combustion chamber. Therefore it is important to determine what going on inside the furnace especially the heat transfer pattern. Heat transfer inside the combustion chamber is governed by the temperature distribution from the flame and the product concentration [1]. For heat to be transferred effectively, the temperature must be distributed uniform throughout the chamber, as the flame give out the heat. However, inside the chamber, there are certain areas that have temperature lower than the distributed temperature. This is due to the presence of NO_x inside the chamber which converts the useful heat into waste heat [2]. Furthermore, the NO_x is a pollutant and can cause corrosion with presence of water vapour. When overall heat transfer is lowered, the combustion efficiency of the furnace or combustion chamber is decreased [3, 4]. However, combustion efficiency is related to the air to fuel ratio, when insufficient air supplied will cause higher amount of uncombusted fuel goes into hydrocarbon emission which lowers efficiency [3, 4]. In other hand, too much air will cool the combustion chamber and carry a larger percentage of the heat out of the flue, reducing combustion efficiency [3, 4]. Therefore, it is important for to know how the temperature are distributed in the event of such conditions which later can be studied in order to achieve better design for furnace and combustion chamber.

1.1.1 Computational Fluid Dynamics

Computational Fluid Dynamics (CFD) is a part of fluid mechanics that applies numerical methods and algorithms in order to solve and analyse problems that relates to flows of fluid. In order to done the calculations, computers are used to compute such task by using specific software that allows complex calculation of a simulation of intended flow process [5]. Using CFD, we can build a computational model that represents a system or device that we want to study. In our case, CFD – FLUENT is used which is a software that uses the science of predicting fluid flow, heat and mass transfer, chemical reactions and related phenomena by solving numerically the sets of governing mathematical equations. The results of CFD analysis are relevant in conceptual studies of new design, detailed product development, troubleshooting and redesigning. Therefore, by using CFD FLUENT, we can build a 'virtual prototype' of the system or device that we wish to analyse and then apply real-world physics and chemistry to the model, and the software will provide with images and data, which predict the performance of that design.

1.1.2 C492 Combustion Lab Unit

The combustion chamber that are used to gather the experimental data for the simulation is C492 Combustion Lab Unit which enables studies into many aspects of combustion and burner operation using the optional burners or any suitable commercially available oil or gas burner up to 150 kW. The four large observation windows fitted in the frame mounted, water cooled, combustion chamber provide an excellent flame demonstration facility. The full instrumentation and safety features allow supervised student operation over a wide range of air/fuel ratios and different fuels [6].

1.2 Problem Statement

Inside today's industrial furnace and combustion chamber, there a lot of uncertainties inside the chamber, especially on flame and temperature distribution. As we all know, air to fuel ratio plays a very important role in determining the combustion efficiency. Too little or too much air will lower the overall combustion efficiency. However, the ones that we do not fully understand are how the temperature is distributed inside the furnace. Therefore, it is important to know how the temperature is distributed inside the chamber and learns how the air to fuel ratio affect the temperature distribution. Hence, we are required to validate the experimental data and compared to the result of simulation through CFD. By validating data from both sets, we can determine the correct methods and models that allows us to implement new design without spent much cost by using CFD simulation software which can reduces the time and operation cost compared to experiments setup and prototyping.

1.3 Objectives

The objectives of this study are:

1. To develop a combustion chamber geometry model using CFD FLUENT in order to simulate the flame and temperature profile inside combustion lab unit C492
2. To validate the simulation results with the experimental results.

1.4 Scope of Study

The scopes of this study are:

1. The scope of this project is to run simulations on temperature distribution and heat transfer pattern inside C492 Combustion Chamber. The limitation of our project is fuel type which is liquid and gaseous fuel. LPG is chosen as only fuel used in the experiment because of majority of today furnaces and combustion chambers use LPG as fuel source. Moreover, the type of LPG used mainly was based on United States' HD – 5 standards. The main compositions of (mass %) were $\text{CH}_4=0.02\%$, $\text{C}_2\text{H}_6=0.95\%$, $\text{C}_3\text{H}_8=98.35\%$, $\text{C}_4\text{H}_{10}=0.67\%$. For the case study, the fuel inlet temperature and air inlet temperature is at ambient temperature of 296 K [7]
2. The simulation model geometry is designed in simplified geometry which is enough to cover the intended objectives. As for the flow and mass transfer, the balance equations used are standards in the CFD – FLUENT 6 and used the Reynolds Average Navier – Stokes (RANS) formulation [5, 8]. Furthermore, the fluid or the fuels are assumed to be Newtonian, and to follow the perfect gas law. The $k - \epsilon$ are used as closure equations and standards value for constants are adopted. [5, 8]. The state of the overall process is considered to be steady state process.
3. To validate the simulation result, we compared the composition of flue gas from the experiment with the simulation data. The simulation result is expected to converge within acceptable error of the actual result.

1.5 Rationale and Significance

The importance of this study is to validate the simulation results with the actual experimental results. If the simulation results fit the actual experimental results, it means that we can test our objectives through simulation instead of doing the expensive actual experiment. This enables us to forecast and analyse data before put to the actual experiment. Therefore, we can significantly improve the design and reduce cost for fabrication of prototype.

CHAPTER 2

LITERATURE REVIEW

This chapter provide a literature reviews with relations to the past research effort such as journals or articles related to combustion process, effect of air/fuel ratio on combustion efficiency of LPG fuel and computational fluid dynamics (CFD) analysis whether on two dimension and three dimension modelling. Moreover, reviews on other relevant studies are made in order to relate to our project.

2.1 Mathematical Modelling of NO_x Emission from High Temperature Air with Nitrous Oxide Mechanism

Previous studies show that the modelling of NO_x emission in term of excess air ratio and temperature distribution. Figure 2.1 depicts the results from experimental measurement and simulation prediction. The experimental results were taken at the burner outlet and the chimney of the furnace. The graph is based on effect of excess air ratio which consists of actual measured results, predicted simulation result with N₂O route and predicted simulation result without N₂O route. The simulation result without the N₂O route is lower than both of measured and prediction with N₂O route. The reason is that when the N₂O route is not present, the simulation assumed that mixing rate was considered complete at excess air ratio equal to 1.04 which allows no formation of NO. As the excess air ratio increases, the temperature increases to which point it allow the simulation to predict the value of NO emission. The simulation with N₂O route shows that NO was formed at lower excess air which corresponds to the measured experimental result which shows NO

formation at every excess air ratio. When comparing with experimental data, the model with N_2O route shows a very good agreement when excess air ratio is equal or less than 1.15. On the other hand, when excess air ratio is equal to 1.25, NO emission is almost two times higher than experimental data. [9]

The result is related to Figure 2.2 which shows the experimental data on the effect of excess air ratio on the maximum temperature, the graph shows that with increasing amount of excess air ratio will increase the maximum temperature of the furnace. It is in fact that oxygen concentration in reaction zone increases as excess air ratio increase which results in a higher flame temperature [9]. It is worth to note that the furnace model used was semi industrial furnace with HiTAC system compared to the one used in this study. Nonetheless, the parameter applies to furnace and combustion chamber in general. Therefore, the results from the literature can be used as base for this project.

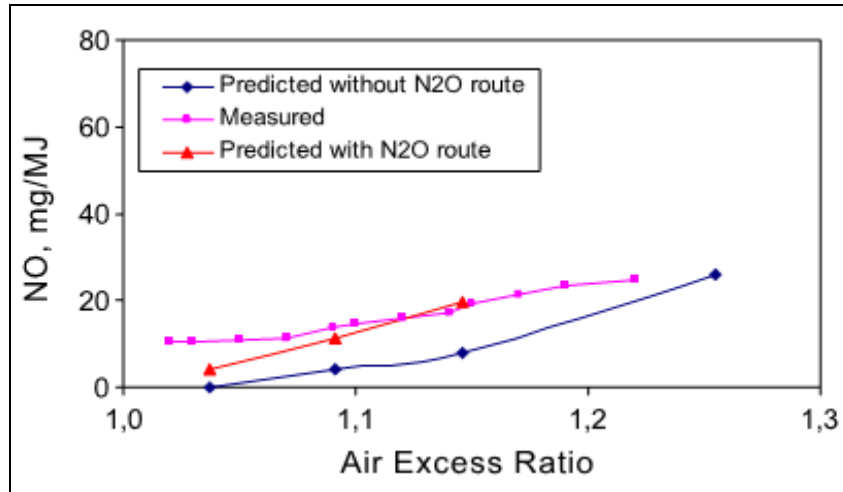


Figure 2.1: Effects of excess air ratio on NO emission.

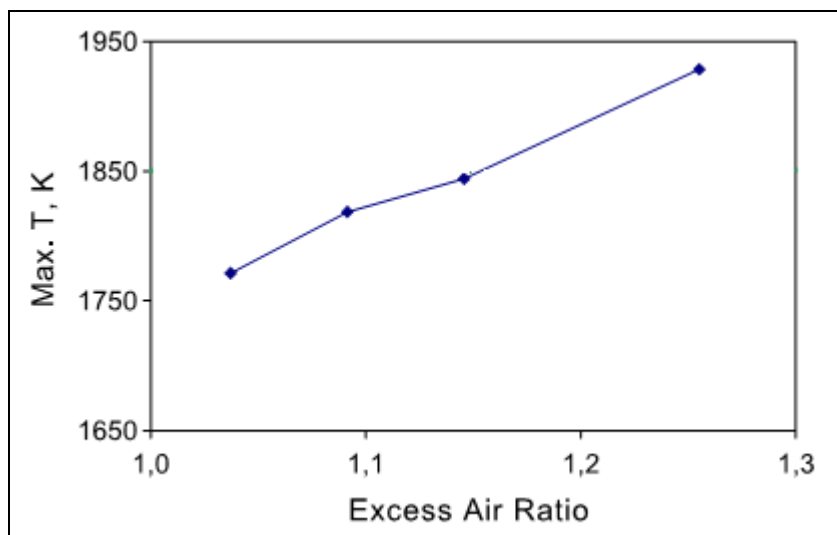


Figure 2.2: Effect of excess air ratio on maximum temperature.

2.1.1 Effects of NO Model on the NO Formations

In order to further understand the effects of the NO model on NO formation and destruction inside furnace or combustion chamber is by investigating temperature profiles as shown in Figure 2.3 which the cross section of the furnace at different excess air ratio. There is usually large chemical reaction zone in all case which can be verified by experimental studies. The highest temperature usually occurs at the middle of the furnace which is where the flame situated. This literature uses HiTAC burner which mix the fuel and combustion air at initial stage of the combustion which also the same operation for the C492 gas burner that is used in this study. The combustion product is entrained into the root of flame because of high injection momentum which reduces the oxygen availability in the primary combustion zone. The unburnt fuel that escaped the primary combustion zone gradually mixed with air to complete the combustion, resulting in more uniform temperature profile. So that, the production rate of NO is lowered. [9]

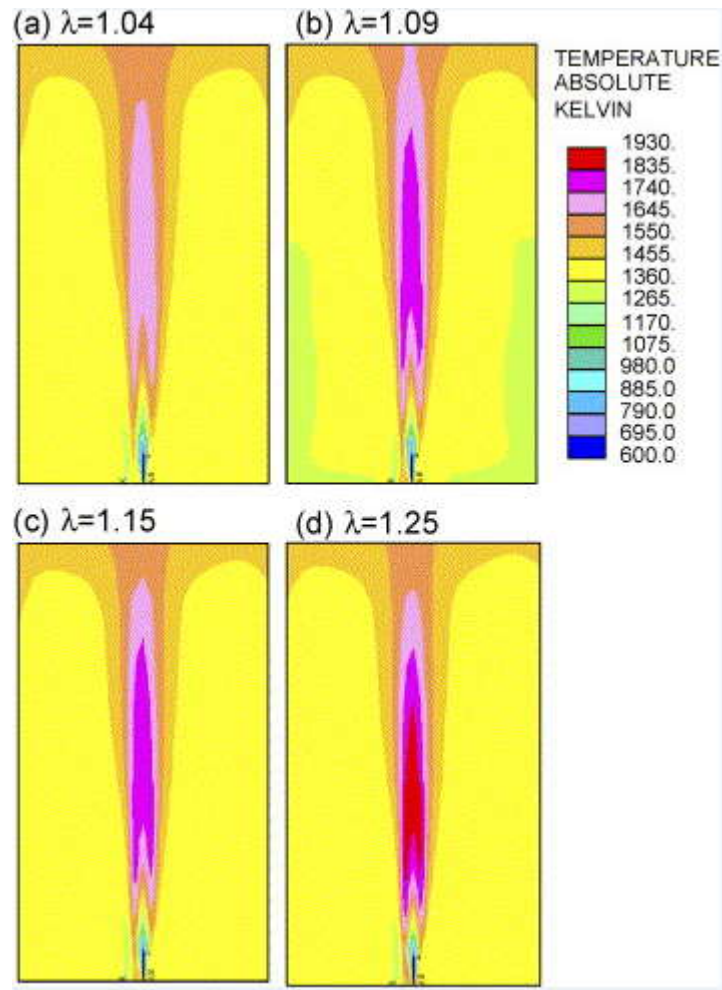


Figure 2.3: Temperature distribution at the cross section through fuel and one air nozzle in the test furnace at different excess air ratio (λ).

The literature concludes that they developed the N_2O route in order to predict the NO formation and emission inside combustion chamber. The results show that the NO emission formed by N_2O intermediate mechanism is important in furnaces that have low peak temperature. Moreover, the increasing excess air ratio leads to increasing NO emission under high temperature air combustion condition.

2.2 Summary of Previous Studies

Table 2.1 below summarized the findings and review others previous work which related to this research.

Table 2.1: Summary of Literature Review

Authors and Year	Study Parameter	Results and Findings
Weihong Yang, and Wlodzimierz Blasiak., 2005[10]	1. Properties of LPG flame 2. Effect of air/fuel ratio on test furnace	1. Size and shape matches the observed flame in test furnace 2. Increasing excess air ratio leads to increasing NO emission
Weihong Yang, and Wlodzimierz Blasiak., 2005[9]	1. NOx emission profile 2. Effect of excess air ratio on NOx emissions	1. Lower excess air ratio leads to larger flame volume and larger entrainment ratio, thus reducing NO emissions
Nabil Rafidi, and Wlodzimierz Blasiak., 2006[11]	1. Heat transfer characteristic inside test furnace 2. Temperature distribution profile	1. Enhancement of temperature and heat flux uniformity. 2. Uniform temperature distribution reduce NOx level inside test furnace

2.3 Combustion Theory

Combustion is defined as burning or in chemical terms as rapid mixture of flammable substance with oxygen which accompanied by the evolution heat of in form of light radiation. Combustion process is an exothermic reaction which is the heat energy from the reaction is given out. As clear example of combustion is a slow burning of candle flame and the explosion of petrol vapour in air [12].

There are six types of combustion process, which are rapid, slow, complete, turbulent, microgravity and incomplete combustion. In rapid combustion, the process releases high amount of heat and energy. In addition, some large amount gaseous will also be produced from the combustion resulting in excessive pressure build-up which

eventually create high noise event called explosion [12]. On contrary, slow combustion occurs at very low temperature which often correlates to the cellular respiration as example. Turbulent combustion is a process where the combustion process is characterized by turbulent flow which helps the mixing between the oxidizer and the fuel producing complete combustion. On other part, microgravity combustion is a combustion process that occurs at low gravity or no gravity condition and often produces spherical flame which is important in understanding combustion physics in space [12].

Complete combustion is a process where the reactant will burn completely in air or oxygen producing limited number of products. In common sense, hydrocarbons which consists of hydrogen and carbon combust with oxygen producing carbon dioxide and water. It's also applies to elements such as nitrogen, sulphur and iron which when are burned will yield common oxides [12]. Complete combustion is also referred as stoichiometric combustion which the theoretical air supplied at exact amount.

Incomplete combustion occurs when air or oxygen supplied is not enough for reactant to completely consume in the reaction or when heat sinks quenched the combustion process. When incomplete combustion happens, the part of the reactant remained unoxidized which will produce additional or unwanted combustion products which mostly are pollutants. The pollutants that may arise from such conditions are carbon monoxides, nitrogen oxides or even sulphur oxides. The increased level of the pollutants means that the flue gas from the combustion can be dangerous and toxic to living things. Moreover, incomplete combustion greatly reduces the heat transfer process and reduces overall combustion efficiency [12].

In actual practice, air is supplied in excess of that of theoretical requirement in order to ensure complete combustion. Excess air can be expressed as percentage of theoretical air needed i.e. 10% excess air is equivalent to 1.1 times of theoretical air quantity. By supplying excess air, the quantity of fuel being wasted is reduced and the variations in fuel quality or air can still be tolerated and guaranteed a complete combustion [4].

2.3.1 Combustion Efficiency

The key to combustion efficiency is the control of excess air ratio. In which when too little will cause incomplete combustion with the pollutants emission, whilst too much will cool the combustion chamber and carry a larger percentage of the heat out of the flue, reducing combustion efficiency. Therefore, combustion efficiency is a calculation of how well your equipment is burning a specific fuel, shown in percent. Complete combustion efficiency would extract all the energy available in the fuel. However 100% combustion efficiency is not realistically achievable. Common combustion processes produce efficiencies from 10% to 95%. Combustion efficiency calculations assume complete fuel combustion and are based on three factors: [3]

1. The chemistry of the fuel.
2. The net temperature of the stack gases.
3. The percentage of oxygen or CO₂ by volume after combustion.

$$n_c = f(\text{airflow rate})^{-1} (1/\text{evaporation rate} + 1/\text{mixing rate} + 1/\text{reaction rate})^{-1}$$

Combustion efficiency also can be expressed as above as the total time required to burn a liquid fuel is the sum of the times required for fuel evaporation, mixing of fuel vapour with air and combustion products, and chemical reaction which relates that time available for combustion is inversely proportional to the airflow rate [3].

2.4 Air Fuel Ratio

The surrounding air consists of 21% oxygen that play major role in combustion and 79% nitrogen which inert that takes no part in combustion process at low temperature. Air is the primary sources of oxygen which is plenty but when it enters combustion process, due to presence of nitrogen, much of the heat of the process is wasted. This is a basic inefficiency which has to be accepted as there is no

economical way of separating the oxygen and nitrogen. Therefore, the ratio of which air and fuel is to be taken into combustion process very important in which it determines the overall efficiency. Air-fuel ratio (AFR) can be defined as the mass ratio of air to fuel present during combustion. When all the fuel is combined with all the free oxygen, typically within a vehicle's combustion chamber, the mixture is chemically balanced and this AFR is called the stoichiometric mixture. AFR is an important measure for anti-pollution and performance tuning reasons. Lambda (λ) is an alternative way to represent AFR. [4]

2.4.1 Effect of Excess Air Ratio

All hydrocarbon fuel has a condition of perfect combustion, in which all the oxygen in the air is consumed, but without excess air. In practice, to ensure complete combustion, excess air is supplied beyond that theoretically required for full oxidization of the fuel. This express as a percentage of the theoretical air needed i.e. 10% excess air is 1.1 times the theoretical air quantity. Having excess air ensures no fuel is wasted, and variations in fuel quality or air and fuel rates can be tolerated and still guarantee complete combustion. The stoichiometric air/fuel ration is different for each fuel because it depends on its chemical composition. In Appendix B, the table of stoichiometric condition of typical fuels is described. Therefore, in the combustion chamber, the effect of excess air ratio plays very important role in combustion efficiency.

2.5 Liquefied Petroleum Gas (LPG)

Liquefied Petroleum Gas (LPG) is a mixture of hydrocarbon gases which primarily consists of butane, propane or methane in certain ratio. LPG is used as fuel sources in heating appliances and vehicles. Common LPG ratios are 60% propane and 40% butane which often depend on season change. Other components in LPG are odorant such as ethanethiol and small concentration of propylene or butylenes.

LPG is synthesized by refining petroleum or extracted from wet natural gas. Wet natural gas meant that the natural gas still contain high amount of heavier hydrocarbons than methane. Although LPG is not renewable fuel, however its advantages weighed more and becoming more popular choice presently. The advantages of LPG are its burns cleanly with no soot or sulphur emission, posing no ground or water pollution hazard and it contains much higher heating value than diesel or gasoline. LPG has a typical specific caloric value of 46.1 MJ/kg compared to 42.5 MJ/kg for diesel and 43.5 MJ/kg for gasoline. However, LPG's energy density per unit volume is much lower than diesel and gasoline which correlates to the volume that LPG can be stored in same container in comparison of diesel and gasoline [7].

The commercialized LPG is in liquid state inside pressurized steel containers or cylinders because at normal temperature and pressures, the LPG will evaporate. However, the LPG is not filled completely in its container to allow thermal expansion of the gases in between 80% to 85% of their filled capacity. The common volume ratio between vaporised gas and the liquefied gas is about 250:1 but it also varies depend on composition, pressure, and temperature. The pressure inside the container is called vapour pressure which depends on LPG composition and pressure i.e. approximately 2.2 bar for pure butane at 68°F and 22 bar for pure propane at 131°F. The density of LPG is much higher than air which means it will settle down on the ground which causes dangerous hazards such as suffocation or explosion if there is source of ignition. [7]

2.6 Background of Study

This section describes the background of study which consists of the explanation on software and equipment used to complete this project. The software principle is presented along with information regarding to the software. The equipment used to done the experiment also is presented.

2.6.1 Computational Fluid Dynamics (CFD)

Computational fluid dynamics is part of fluid mechanics that uses numerical method and algorithm to solve and analyse problem that related to fluid flow. This section describes the definition, history and the advantage of using computational fluid dynamics.

2.6.1.1 Definition of CFD

CFD is a computer-based mathematical modelling tool that incorporates the solution of the fundamental equations of fluid flow, the Navier-Stokes equations, and other allied equations. CFD incorporates empirical models for modelling turbulence based on experimentation, as well as the solution of heat, mass and other transport and field equations. In order to done the calculations, computers are used to compute such task by using specific software that allows complex calculation for simulation of intended flow process. There are three phases to CFD: pre-processing, or creation of a geometry usually done in a CAD tool; mesh generation of a suitable computational domain to solve the flow equations on; and solving with post processing, or visualization of a CFD code's predictions. CFD is now a widely accepted and validated engineering tool for industrial applications. In our case, CFD – FLUENT is used which is a software that uses the science of predicting fluid flow, heat and mass transfer, chemical reactions and related phenomena by solving numerically the sets of governing mathematical equations. The results of CFD analysis are relevant in conceptual studies of new design, detailed product development, troubleshooting and redesigning [5, 8].

2.6.1.2 History of CFD

It is debatable as to who did the earliest CFD calculations (in a modern sense) although Lewis Fry Richardson in England (1881-1953) developed the first numerical weather prediction system when he divided physical space into grid cells and used the finite difference approximations of Bjerknes's "primitive differential equations". His own attempt to calculate weather for a single eight-hour period took six weeks of real time and ended in failure! His model's enormous calculation requirements led Richardson to propose a solution he called the "forecast-factory". The "factory" would have involved filling a vast stadium with 64,000 people. Each one, armed with a mechanical calculator, would perform part of the flow calculation. A leader in the centre, using coloured signal lights and telegraph communication, would coordinate the forecast. What he was proposing would have been a very rudimentary CFD calculation.

During the 1960s, the theoretical division of NASA at Los Alamos in the U.S. contributed many numerical methods that are still in use in CFD today, such as the following methods: Particle-In-Cell (PIC), Marker-and-Cell (MAC), Vorticity-Stream function methods, Arbitrary Lagrangian-Eulerian (ALE) methods, and the ubiquitous $k - \epsilon$ turbulence model. In the 1970s, a group working under D. Brian Spalding, at Imperial College, London, developed Parabolic flow codes (GENMIX), Vorticity-Stream function based codes, the SIMPLE algorithm and the TEACH code, as well as the form of the $k - \epsilon$ equations that are used today (Spalding & Launder, 1972). They went on to develop Upwind differencing, 'Eddy break-up' and 'presumed PDF' combustion models. Another key event in CFD industry was in 1980 when Suhas V. Patankar published "Numerical Heat Transfer and Fluid Flow", probably the most influential book on CFD to date, and the one that spawned a thousand CFD codes.

It was in the early 1980s that commercial CFD codes came into the open market place in a big way. The use of commercial CFD software started to become accepted by major companies around the world rather than their continuing to develop in-house CFD codes. Commercial CFD software is therefore based on sets of very complex non-linear mathematical expressions that define the fundamental

equations of fluid flow, heat and materials transport. These equations are solved iteratively using complex computer algorithms embedded within CFD software. The net effect of such software is to allow the user to computationally model any flow field provided the geometry of the object being modelled is known, the physics and chemistry are identified, and some initial flow conditions are prescribed. Outputs from CFD software can be viewed graphically in colour plots of velocity vectors, contours of pressure, lines of constant flow field properties, or as "hard" numerical data and X-Y plots.

CFD is now recognized to be a part of the computer-aided engineering (CAE) spectrum of tools used extensively today in all industries, and its approach to modelling fluid flow phenomena allows equipment designers and technical analysts to have the power of a virtual wind tunnel on their desktop computer. CFD software has evolved far beyond what Navier, Stokes or Da Vinci could ever have imagined. CFD has become an indispensable part of the aerodynamic and hydrodynamic design process for planes, trains, automobiles, rockets, ships, submarines; and indeed any moving craft or manufacturing process that mankind has devised. [13]

2.6.1.3 Advantages of CFD

Nowadays, CFD simulation software is widely used across the world in many sectors. Wide range of application is used in CFD to simulate in the lot of the aerospace, nuclear and automotive sectors through manufacturing, chemical and process sectors to the pharmaceuticals, biomedical and electronics industries.

The advantages using this software:

1. This software allows us to make changes to the analysis at any time during the setup, solution, or post processing phase. This saves time and enables us to refine our designs efficiently. The intuitive interface makes learning easy. Smart panels show only the modelling options that are appropriate for the problem setup at hand. Computer aided design (CAD) geometries are easily

imported and adapted for CFD solutions.

2. Solver enhancements and numerical algorithms that decrease the time to solution are included in every new release of our software. Our mature, robust, and flexible parallel processing capability enables us to solve bigger problems faster, and has been proven on the widest possible variety of platforms in the industry.
3. FLUENT's post processing provides several levels of reporting, so we can satisfy the needs and interests of all audiences. Quantitative data analysis can be as rigorous as we require. High resolution images and animations allow us to communicate our results with impact. Numerous data export options are available for integration with structural analysis and other computer aided engineering (CAE) software programs.

2.6.2 C492 Combustion Lab Unit

This unit enables studies into many aspects of combustion and burner operation using the optional burners or any suitable commercially available oil or gas burner up to 150 kW. The four large observation windows fitted in the frame mounted, water cooled, combustion chamber provide an excellent flame demonstration facility. The full instrumentation and safety features allow supervised student operation over a wide range of air/fuel ratios and different fuels [6]. Figure 2.4 depicts the picture of the combustion chamber.



Figure 2.4: C492 Combustion Lab Unit [6]



Figure 2.5: Control Panel of C492 Combustion Lab Unit [6]

2.6.2.1 C492 Combustion Lab Unit Configuration

The C492 Combustion Lab Unit used in this study is equipped with two interchangeable one-flame burner systems which is one is for liquid fuel and the another is for gaseous fuel. The overall dimension of the Lab Unit are 1560mm(height) x 800mm(width) x 1800mm(depth) and the weight are 250kg for 220V unit(260kg for 110V unit)[6]. The frame is powder coated 25mm mild steel angle frame with 16 swg shelves on which the combustion chamber is mounted. The stainless steel chamber is mounted horizontally on the frame and has a water jacket around the outside and at the rear end through which mains water passes to remove heat produced from the burner. At the front end is the burner mounting plate which has studs onto which either gas or oil burners can be mounted. The inside of the plate has insulation to prevent excessive heat exposed to the operator's position. There are 2 circular high temperature glass windows along side the chamber for which the flame can be observed.

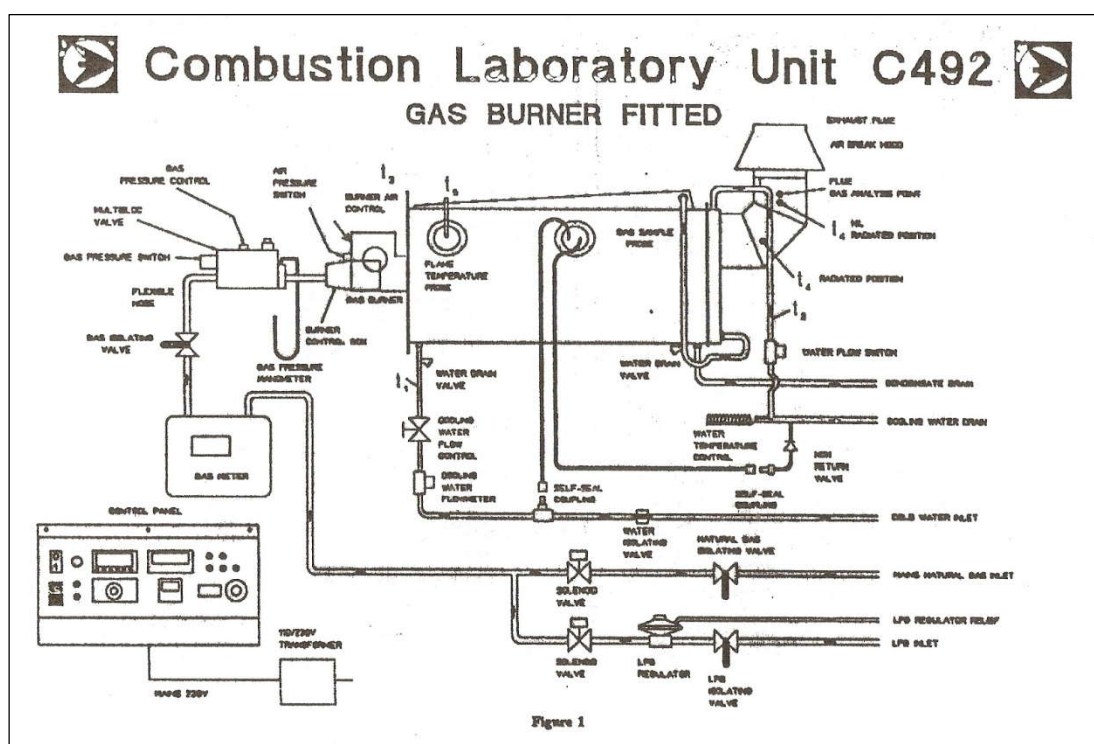


Figure 2.6: Schematic Diagram of Gas Burner fitted on C493 Combustion Lab Unit.

The dimensions of the stainless steel combustion chamber are 450mm ID @ 500mm OD x 1000mm long with four 100mm diameter quartz glass window. The front plate has 80mm thick insulation and burner mounting stud. At the rear end, there is one flue gas duct of 150mm OD for removing the hot flue gas from the combustion chamber which goes through an insulated 90° bend section. At this section, there are tapping points which exhaust thermocouple, air and gas analyser sensor probe can be inserted. An air break hood is installed to the flue duct to entrain ambient air and to cool the flue gases. Condensate that may collect within the chamber is drained away from a point towards the rear of the chamber [6].

A 150kW one-flame C492A Gas Burner is used in this study. The one flame gas burner features one fuel nozzle surrounded by air inlets and fuel gas outlet. The fuel and the air is injected directly into the combustion chamber at high velocities which the strong entrainment led by these injection moment will cause the combustion air to be well mixed with the fuel.

CHAPTER 3

METHODOLOGY

3.1 Overall Research Methodology

The flow charts in Figure 3.1 shows the overall research methodology of this project. Numerical approach will be used to solve the three dimensional analysis of C492 Combustion Lab Unit. The boundary condition is taken from the experimental data. Excess air ratio is the main parameter data will be validated at the early stages and the effect of excess air ratio on combustion efficiency will be directly compared on later stages.

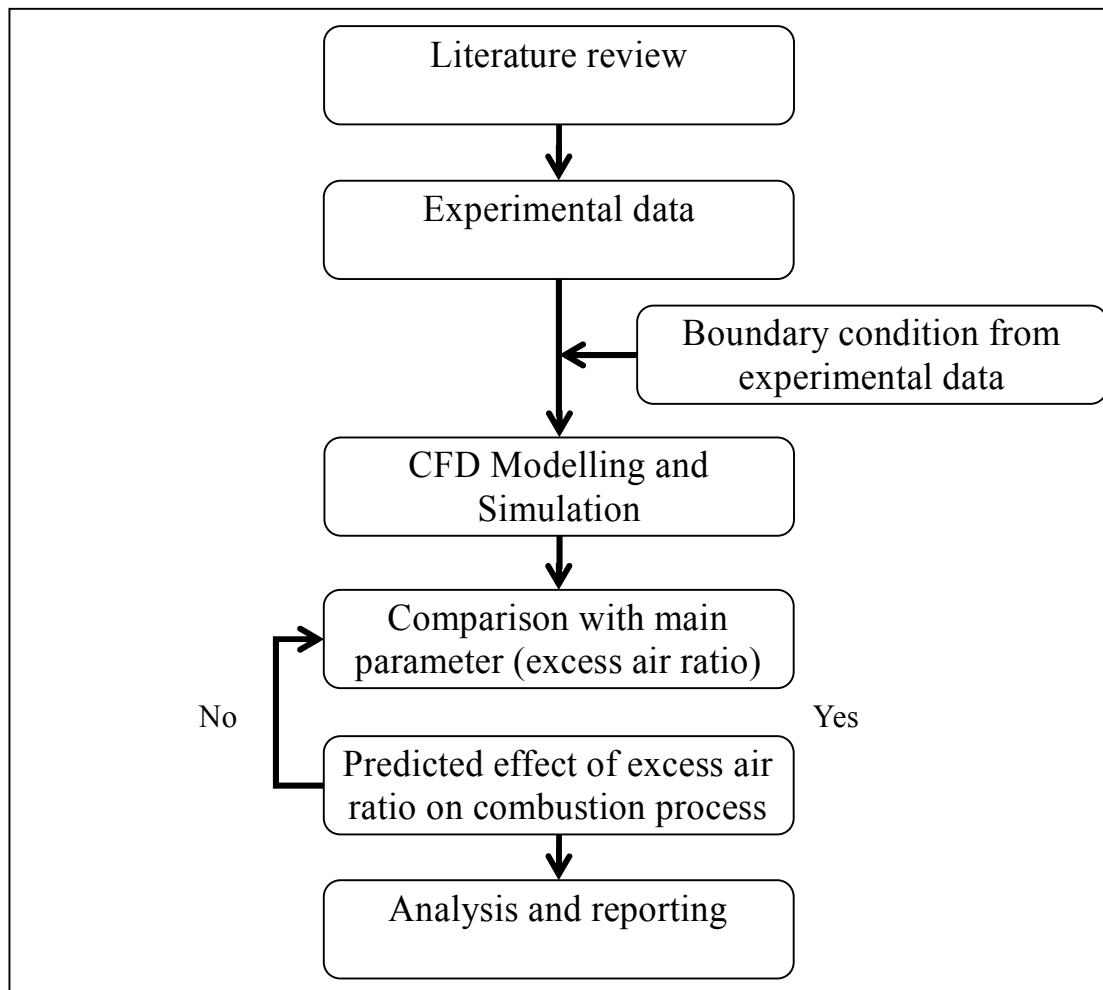


Figure 3.1: Flow charts of research methodology.

3.2 CFD Modelling and Simulation

CFD – FLUENT 6 is used for the modelling and simulation in this project. CFD – FLUENT 6 is computer software that allows modelling and simulation of flow of fluid and heat and mass transfer in complex geometries. It is capable to complete meshing flexibility, solving flow problems with unstructured meshes that can be generated through the complex geometries. The program structure is shown in Figure 3.2.

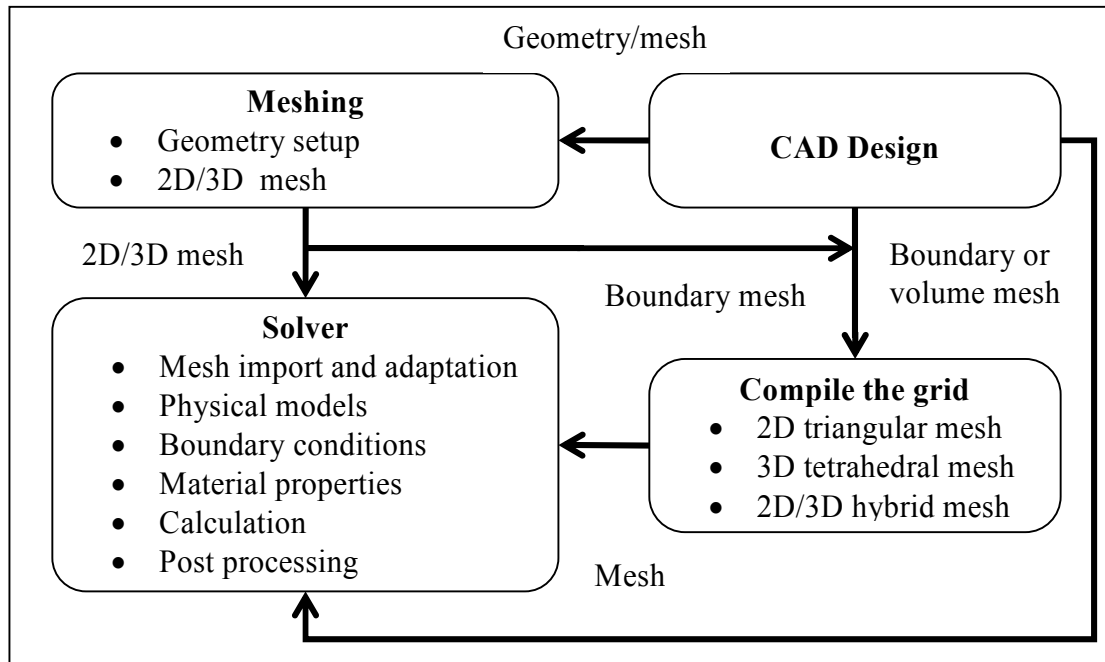


Figure 3.2: Program Structure.

3.3 Problem Solving Steps

By using the CFD – FLUENT 6, the problem solving steps involves the problem identification, grid creation, solver execution and analysis of the result. The advantages is given by its build in post processing that enables automatic save on setting file data written in *.dat or *.cas file. The detailed steps are shown in Figure 3.3.

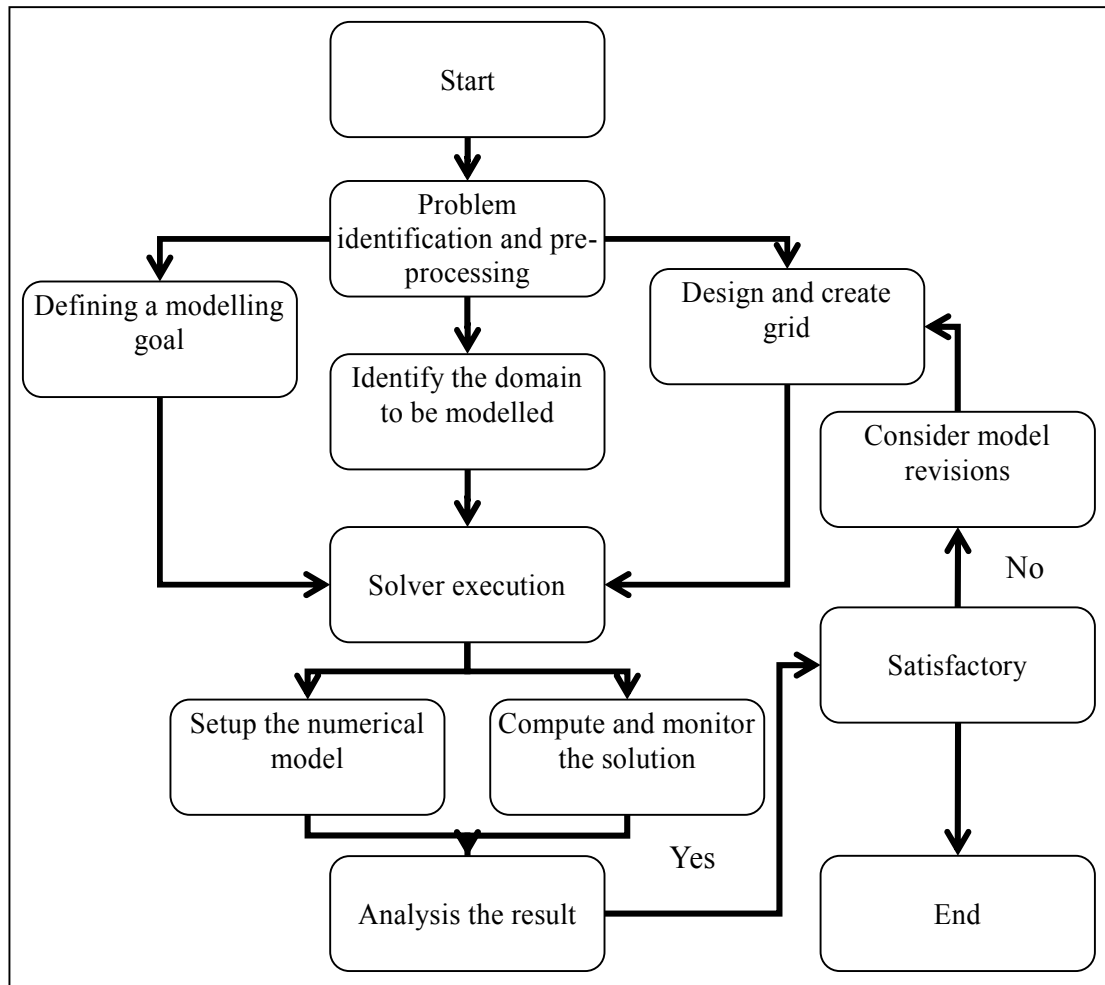


Figure 3.3: Steps of CFD analysis.

3.3.1 Geometry Design/Meshing Geometry – GAMBIT

In order to create a suitable model to run in FLUENT software, pre-design geometry must be created to match with the needs of FLUENT. Therefore, GAMBIT which is a geometric modelling and grid generation tool is provided along with the FLUENT technology. GAMBIT allows the user to import geometry from other designing software or computer-aided design (CAD) software or create own geometry entirely based on GAMBIT itself. In addition, GAMBIT can automatically mesh surfaces and volume while allowing the user to manipulate the mesh through size functions and boundary layer meshing.

3.3.1.1 The Combustion Chamber Geometry and Materials

The wall of the combustion chamber is made of stainless steel which is inside stainless steel water jacket. The wall thickness is about 10 mm and the gap between the walls with the water jacket is about 25 mm. The length of the combustion chamber is about 1060 mm including the water jacket. The diameter of the chamber is about 500 mm including the water jacket. The gas burner head consist of a air nozzle and fuel nozzle that made of high temperature alloy. The fuel inlet is about 10 mm in diameter and the air inlet is the annulus of the fuel inlet which is about 35 mm in diameter. Figure 3.4 depicts the overall dimension without including the water jacket dimension.

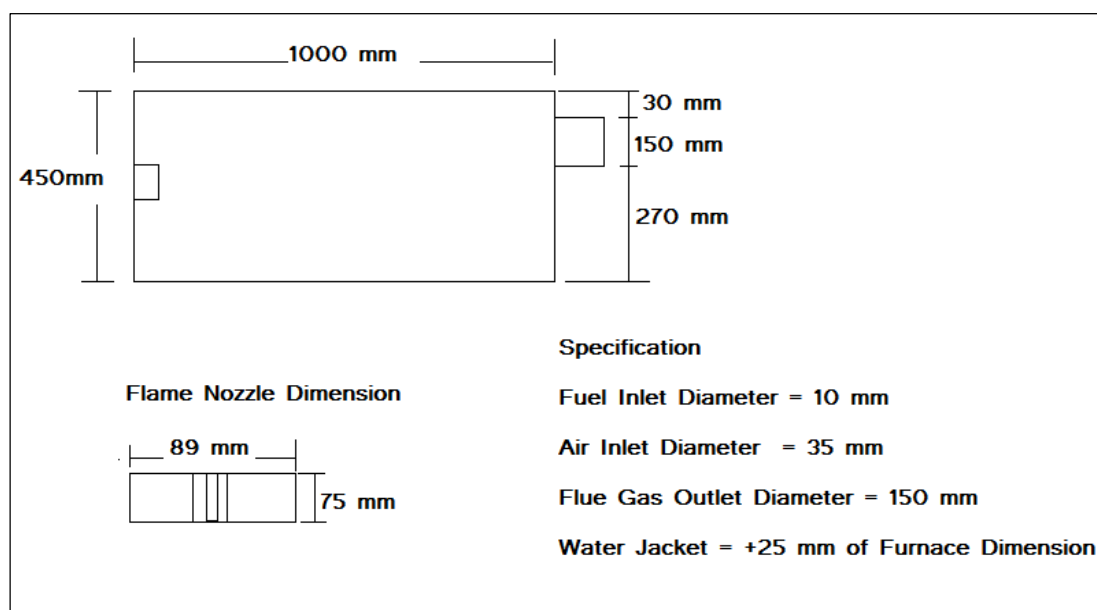


Figure 3.4: Overall combustion chamber dimension.

3.3.1.2 Combustion Chamber Meshing

The simplified geometry of combustion chamber consist of 6 cylindrical volume that has been stitched together to produce a single volume as in Figure 3.5. The stitched volume that created the geometry of chamber consists of 100,000

elements. After a series of trial and error, the grid independency tests stabilize at nearing 100,000 elements under the scheme of Tet/Hybrid element and TGrid type meshing. The wall meshing was set to have First/Last ratio and element about 100 interval counts. The outlet flue mesh was decomposed first to allow the mesh to link together. The face meshing was done of circle faces of the chamber. The face meshing uses Quad element and Pave type scheme. After the meshing was complete, boundary condition was defined as follow:

1. Fuel Inlet - Velocity Inlet
2. Air Inlet - Velocity Inlet
3. Flue Outlet - Pressure Outlet
4. Furnace walls - Wall
5. Gas Nozzle - Wall

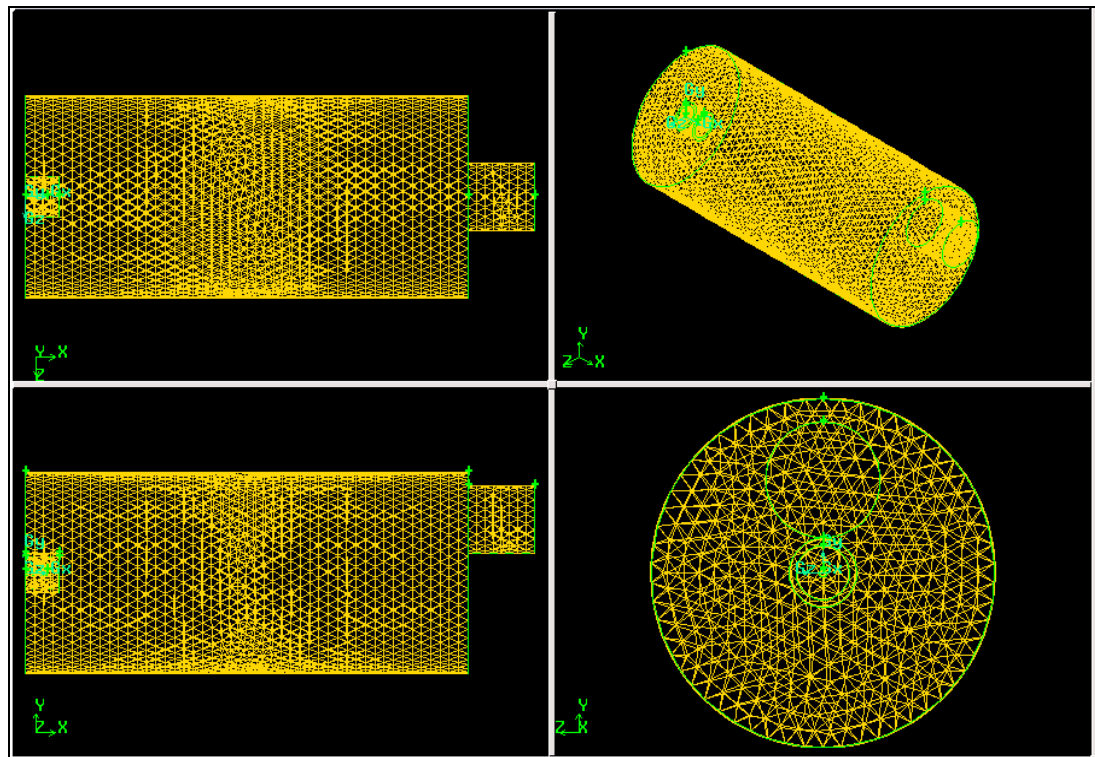


Figure 3.5: Meshed combustion chamber geometry.

3.3.2 FLUENT Simulation

This part describes the general concepts and theory related to using computational fluid dynamics (CFD) to analyse fluid flow and heat transfer, as relevant to this research. It starts with review of the tools needed for carrying out the CFD analyses and the processes required, followed by a summary of the governing equations and turbulence models (with details given in Appendix A: CFD Computational Tools) and finally a discussion of the discretisation schemes (details in Appendix A: CFD Computational Tools) and solution algorithms is presented.

3.3.2.1 CFD Computational Tools

In order to solve the intended simulation model, one must required a CFD software that are capable to achieve the solution and hardware that contains these element which are pre-processor, processor and post-processor capabilities [Appendix A].

In this research project, commercial CFD software codenamed FLUENT was used to solve the objective of the research by simulate the intended simulation model. The geometrical design and meshing was done on notebook and partial trial and error simulation calculation done in order to achieve the correct model. The notebook used was Compaq Presario with dual processors totalling 2.3 GHz RAM, running on Microsoft Vista Operating System. The GAMBIT software was used to geometry construction and meshing was packaged along with FLUENT software. FLUENT was used for the CFD calculations. The calculations were carried out approximately 100,000 elements. The time taken for calculation based on steady state solver took between 2 – 3 hours to finish the calculations, if were done based on unsteady state solver, the simulations could took 2 – 3 days running in parallel on both processors. Therefore, after the suitable model was achieved, the simulation model was transferred to workstation that capable of running several processors in parallel to reduce the time for iterations.

3.3.2.2 FLUENT Governing Equations

The FLUENT consist of fundamental governing equations to mathematically solve for fluid flow and heat transfer, based on the principles of conservation of mass, momentum, and energy. The conservation equations are described in Appendix A: CFD Computational Tools which tells that how it is applied in CFD calculations.

3.3.2.2.1 Conservation Equations

The conservation laws of physics form the basis for fluid flow governing equations (describes briefly as Equation A.1.1-A.1.9 in Appendix A1: Governing Equations). The laws are:

Law of Conservation of Mass: Fluid mass is always conserved. (Equation A1.1)

$$\frac{\partial(\rho u_i)}{\partial x_i} = 0.$$

Newton's 2nd Law: The sum of the forces on a fluid particle is equal to the rate of change of momentum. (Equation A1.2)

$$\frac{\partial}{\partial x_i}(\rho u_i u_j) = \frac{\partial}{\partial x_i} \left(\mu \frac{\partial u_j}{\partial x_i} \right) - \frac{\partial p}{\partial x_j}.$$

First Law of Thermodynamics: The rate of head added to a system plus the rate of work done on a fluid particle equals the total rate of change in energy. (Equation A1.3)

$$\frac{\partial}{\partial x_i}(\rho u_i T) = \frac{\partial}{\partial x_i} \left(\frac{k}{C_p} \frac{\partial u_j}{\partial x_i} \right).$$

The fluid behaviour can be characterised in terms of the fluid properties velocity vector u (with components u , v , and w in the x , y , and z directions), pressure p , density ρ , viscosity μ , heat conductivity k , and temperature T . The changes in

these fluid properties can occur over space and time. Using CFD, these changes are calculated for small elements of the fluid, following the conservation laws of physics listed above. The changes are due to fluid flowing across the boundaries of the fluid element and can also be due to sources within the element producing changes in fluid properties. This is called the Euler method (tracking changes in a stationary mass while particles travel through it) in contrast with the Lagrangian method (which follows the movement of a single particle as it flows through a series of elements).

3.3.2.3 Turbulence Modelling

In this research project, two turbulence models which are k-epsilon and SST k-omega (the model are discussed further in Appendix A: CFD Computation Tools) are utilized in order to investigate which is best to use for simulation model. After series of trial and errors simulation done, it is found that through k-epsilon model is most suitable to simulate the simplified furnace geometry. The turbulence models that are used are all based on variances of the Reynolds averaged Navier-Stokes (RANS) equations, in which average values for turbulent fluctuations are used for modelling the turbulence.

3.3.2.4 FLUENT Discretisation

The numerical solution procedure is split into two parts. The solution of the flow and the mixing field is performed in a Computational Fluid Dynamics (CFD) code complemented with the nonpremixed combustion. In the CFD code the Favre averaged form of the conservation equations for mass and momentum are solved. Turbulence is modelled by using the standard k-e turbulence model, which involves the solution of transport equations for the turbulent kinetic energy, k , and for its dissipation rate, ϵ .

3-D Segregated model with implicit formulation based on pressure base

solver was selected. The solver conditions are set for steady flow with enhanced wall treatment. Adiabatic conditions are considered at the wall. In order to understand the energy transfer inside the chamber, the energy equation (the equation is described briefly in Appendix A: CFD Computational Tools) was selected and calculation based on convective and radiation model. This however, the radiation model used was the P1 radiation model which described in Appendix A: CFD Computational Tools. The species that take part in the combustion process was set to follow non premix model which are described briefly in Appendix A: CFD Computational Tools. A probability density function (PDF) was set up to follow the fuel composition in order to define the tolerable amount of species can be formed. The operating condition for the simulation was set to follow the experimental data which was at ambient pressure. The boundary condition created in GAMBIT was redefined whereas the specificity of the boundary was set. The input of fuel velocity, air velocity, and the behaviour of which the boundary will react was set. Table 3.1 depicts the boundary condition with velocity inlet, and turbulence intensity.

Table 3.1: Boundary condition

Boundary Condition	Velocity Inlet (m/s)			
Fuel Velocity	10.4	10.4	10.3	10.3
Air Velocity	6.9	7.2	7.5	7.8
Turbulence Intensity	10 %	10 %	10 %	10 %

The solution control was the SIMPLE algorithm that was selected for Pressure – Velocity coupling. First order upwind method was selected for discretisation of momentum, turbulence K.E and turbulence dissipation rate. For pressure, PRESTO! discretisation scheme was selected for pressure. The convergence criterion was set at 0.0000001, as for the iteration process, 1500 iterations was done. Figure 3.6 shows the iteration process.

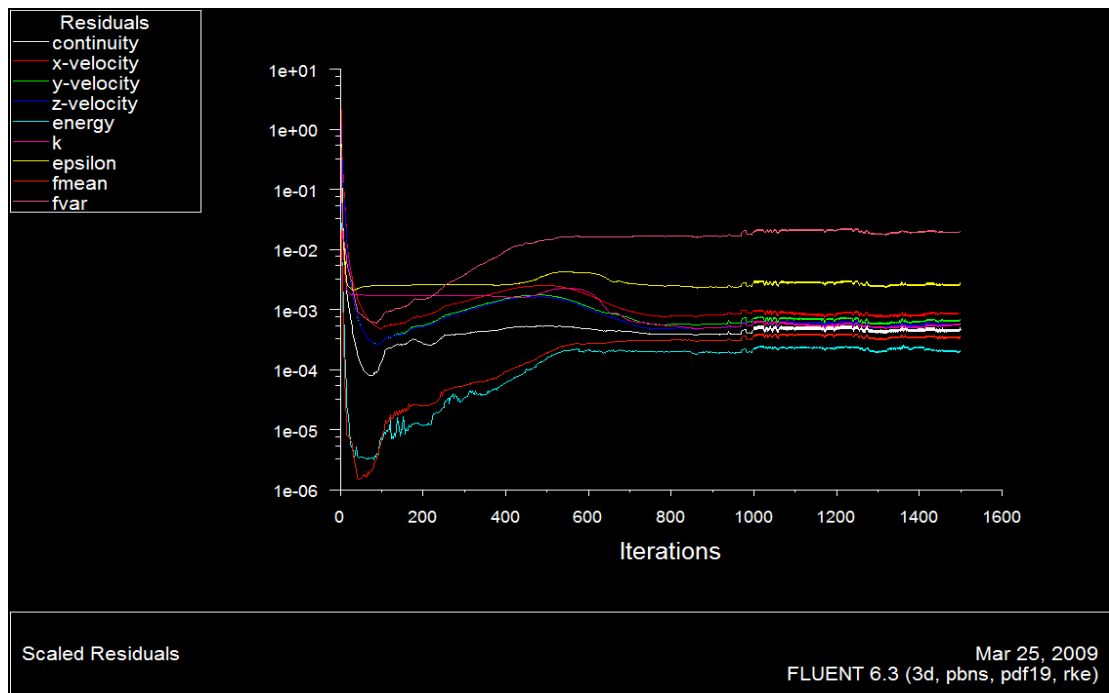


Figure 3.6: Iteration process

The post processing steps was done after the iteration process was complete. From contours or vector view, the model is simulated to get the temperature distribution and heat transfer pattern. The temperature was obtained from the contours and the heat transfer pattern was obtained from alphanumeric data.

3.4 Experimental Methodology

The purpose of the experiment is to provide experimental data which can be used to validate whether the simulation model accuracy. Moreover, the experiment also provides initial input data in order to run the simulation.

The combustion chamber that are used to gather the experimental data for the simulation is C492 Combustion Lab Unit which enables studies into many aspects of combustion and burner operation using the optional burners or any suitable commercially available oil or gas burner up to 150 kW. The four large observation

windows fitted in the frame mounted, water cooled, combustion chamber provide an excellent flame demonstration facility. Figure 2 shows the picture of the combustion chamber. The full instrumentation and safety features fulfil the investigation requirements for the excess air ratio parameter.

The combustion chamber was set to use liquefied petroleum gas (LPG) but based on propane as major constituents as fuel source which uses the gas burner head. The combustion chamber was started by following the operating procedure. After the combustion chamber was started, the gas burner was allowed to fire. The gas burner firing was the preparation step before taking the reading. The gas pressure outlet was set to 116 sec using the gas flow rate timer and the cooling water was adjusted to constant temperature of 60 to 80°C. The firing was allowed to stabilize in order to provide stable flame firing condition. The air damper was adjusted to get the desired excess air ratio. For each excess air ratio, the reading for temperature at flame probe, exhaust probe was taken along with other important reading that need in the calculation. After all desired reading was taken; the gas burner was shutdown and was process to shutdown procedure. Therefore, the list of procedure which needed to be done in order to done the experiment was described as below.

3.4.1 Experimental Methodology Outline

In order to validate our simulation, it is important that we run the experiment in which we can obtain the actual result. Figure 3.7 depicts the flow chart of the experimental methodology.

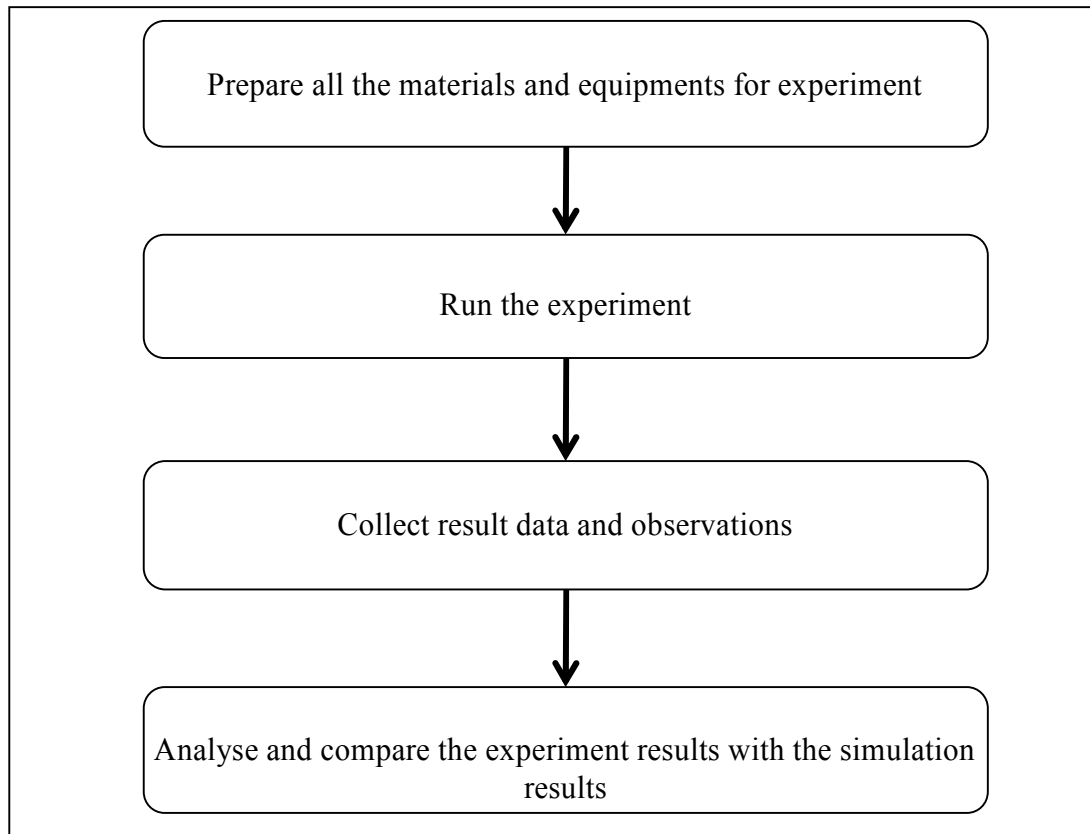


Figure 3.7: Flow chart of experimental methodology.

3.4.2 Materials and Equipments

In order to collect the experimental data, the experiment requires a number of equipment and material. The equipments that were used in this project consist of C492 Combustion Lab Unit, C492A Gas Burner 150kW and C492D Flue Gas Analyser. Meanwhile, the fuel source used for the experiment is LPG.

3.4.3 Operating Procedure

Before the experiment could be carry out, the start up procedure must be done in order to run the experiment. The operating procedure consists of three parts which are preparation, setting up the gas burner and starting up the gas burner. However, the preparation step is only done if the oil burner was mounted on the furnace. The

gas burner is fitted onto the mounting studs and the power plug is connected to its socket. Then, the blanking cap is removed and the flexible hose coupling is screwed to the isolating valve end. When the square plug is connected onto solenoid valve, the pressure manometer tube is connected to the outlet pressure of multibloc valve. The multibloc valve is opened full to allow gas to flow through.

The gas burner is started by switching on the isolator, main switch. Water supply is supplied by opening the main isolating valve and valve at rear unit. The cooling water flow is set to 200g/s. When the flow reaches its point, green signal was given on the panel. The temperature control for cooling water is set at 80°C and the pressure control is set not more than 2 bar. The lever isolating valve is opened to allow gas flow and the burner air control damper is set at position 1-2 so that minimal air is allowed in for the combustion. The chamber is first purged with air by pushing the blower button and allows the pressure to rise at start level. After that, to the mixture of the gas and air is ignited by pressing the burner reset button. To maintain the flame, the gas pressure is adjusted by using the control screw of the gas flow and air flow by using burner air control damper. When the condition has stabled, the experiment is ready to carry out.

3.4.4 Experiment Procedure

When the condition has stabled, the experiment is carry out by setting the gas outlet pressure on the manometer. As stated in the operating procedure, the temperature of cooling water is adjusted and kept constant between 60 to 80 °C. Then, air damper is adjusted to minimum level which sustains the combustion. Again, the condition is allowed to stabilize and the initial reading was recorded. After that, the air damper position is increased by one graduation until it achieve the first excess air ratio. Once more, the condition is allowed to stabilize and the reading is recorded. This step is repeated for other excess air ratio. More over, the experiment is continued to the maximum setting for air flow which when the combustion cannot be sustained. Finally, the burner was shutdown and the data and observation is processed in derived result sheet as in Appendix D: Experimental Data.

CHAPTER 4

RESULTS AND DISCUSSIONS

4.1 Introduction

This undergraduate research project is aimed to achieve its objective which is to develop a simulation model for C492 combustion chamber and validate it with the experimental data in terms of flame temperature, flue temperature, excess air ratio, and energy balance. Besides that, the simulation also shows what experimental data could not show such as temperature distribution inside the chamber and the heat transfer patterns of the combustion process. These criteria have become more important in designing better combustion chamber or furnace with high performances and efficiencies.

The results of excess air ratio by experimental work and CFD simulation are shown in this chapter. The simulation was carried out to obtain temperature at exhaust outlet and at the flame in order to compare with experimental results that were taken at flue probe and flame temperature probe. In this present study, liquefied petroleum gas (LPG) but based on propane properties was used as fuel source, and the fuel flow rate was maintained at a relatively constant flow. The combustion chamber cylindrical dimension is about 1000 mm long, and 450 mm in diameter with a flue outlet of 150 mm diameter. The combustion process was set to utilize excess air ratio as the main parameter which ranged from 1.24 to 1.41.

The simulation results were then compared with the experimental work data in order to validate the model. The simulation result for flue temperature was taken at

outlet of the flue exhaust and the flame temperature was taken at middle point of the flame. The agreements of predicted and measured are very encouraging, especially; the FLUENT simulation shows a very good prediction of the C492 furnace's flame temperature and flue temperature.

4.2 Experimental Results

The experiment was carried out using liquefied petroleum gas based on propane as major constituent as fuel source. The initial parameters are as follow:

- Fuel = Liquefied Petroleum Gas (LPG)
- Ambient Temperature = 296 K
- Ambient Pressure = 1030 mbar
- Stoichiometric Air/Fuel Ratio (by mass) = 15.6
- Density of Gas = 1.8 kg/m³

The constant parameter is the fuel flow rate and the variable parameter is the excess air ratio. The exhaust temperature was obtained from the control panel which read temperature inside the chamber at one point. The flame temperature was obtained from flue outlet probe which are read from the panel. The air/fuel ratio and the heat input was obtained through calculation which described in Appendix D: Calculations. Table 4.1 depicts the summary of the experimental observation and calculation results.

Table 4.1: Experimental Results

Flow rate (by mass), kg/m ³	Excess Air, λ	Exhaust Temperature, K	Flame Temperature, K	Air/Fuel Ratio (by mass), kg/kg	Heat Input (Q _{in}), kW
5.31	1.248	1007	1437	19.47	73.77
5.27	1.299	1003	1436	20.26	73.17
5.23	1.362	1000	1442	21.25	72.58
5.23	1.417	986	1443	22.11	72.58

4.3 Simulation Results

This section describes the result of simulation in term of temperature profile based on different excess air ratio inside the combustion chamber. In addition, the turbulence of the combustion process is also shown.

4.3.1 Temperature profile at side view of the geometry

Figure 4.1 depict the contour of temperature distribution at side view of the furnace geometry. The distribution is based on total temperature and taken at level 20 distribution scheme. Level 20 distribution shows the full distribution of temperature inside the chamber. The temperatures taken at the flame point as shown in the figure 4.2 at level 3 distribution is the initial point when the combustion process started and maintained in the simulation. Meanwhile, the flue outlet temperatures is taken at the outlet point as shown in figure 4.1 at level 20 distribution because it represent the full distribution of temperature at the outlet. Detailed data on the simulation is described in Appendix C: FLUENT Simulation Result.

Figure 4.3 shows the velocity vector of the temperature distribution inside the furnace. It can be seen that the highest velocity of the mixture is in the middle area of the furnace because the mixture started to react and given extra energy by the ignition source. The figure shows that the higher the velocity, the longer the arrow will be. The arrows are coloured based on total temperature which it shows that at area of high temperature, the velocity is high. Moreover, the figure also show the direction of the flow which correspond to the turbulence inside the furnace. The figure represent for excess air ratio equal to 1.248 but it also represent for all excess air ratio. For other excess air ratio is described in Appendix C: FLUENT Simulation Result.

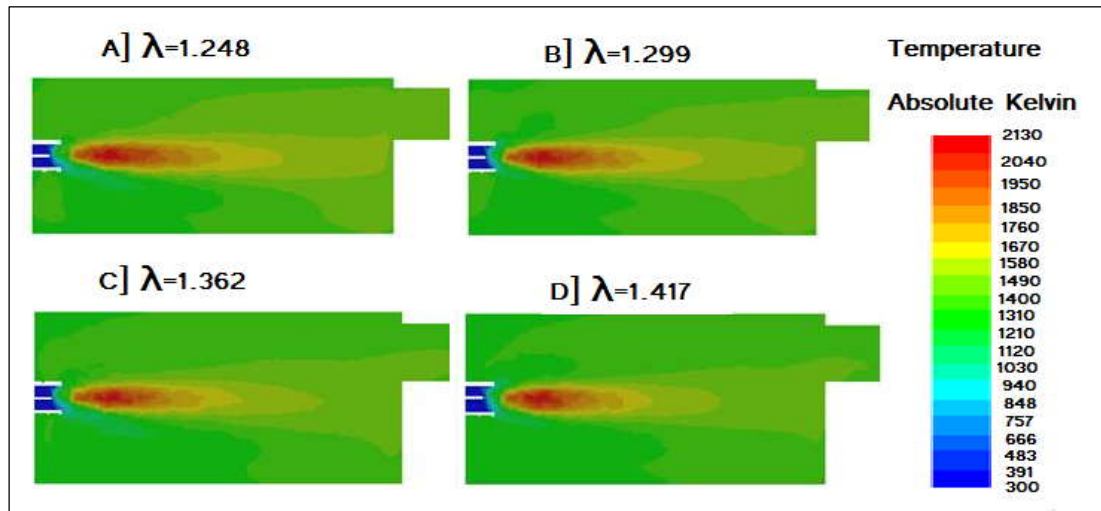


Figure 4.1: Temperature distribution at cross section through fuel and air nozzle in furnace at different excess air ratio (λ) at level 20 distribution.

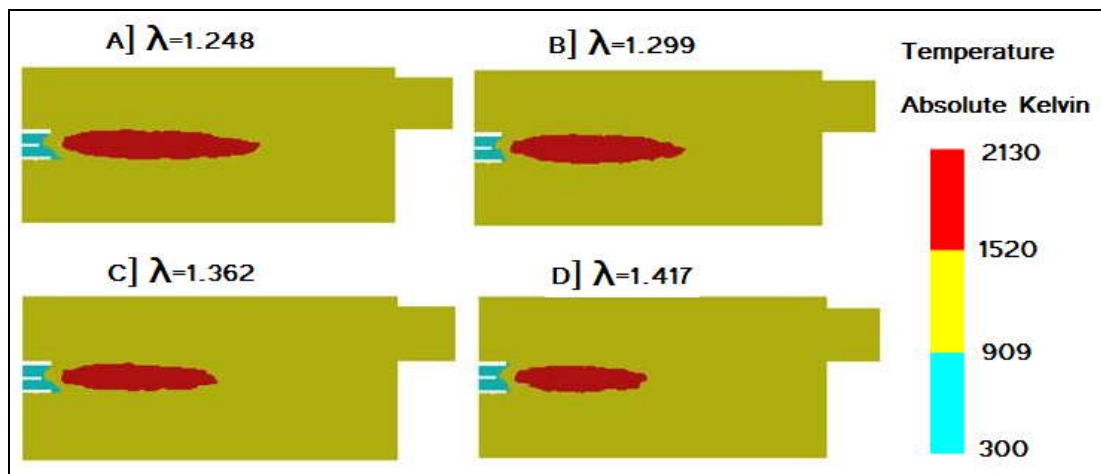


Figure 4.2: Flame cross section through fuel and air nozzle in furnace at different excess air ratio (λ) at level 3 distribution.

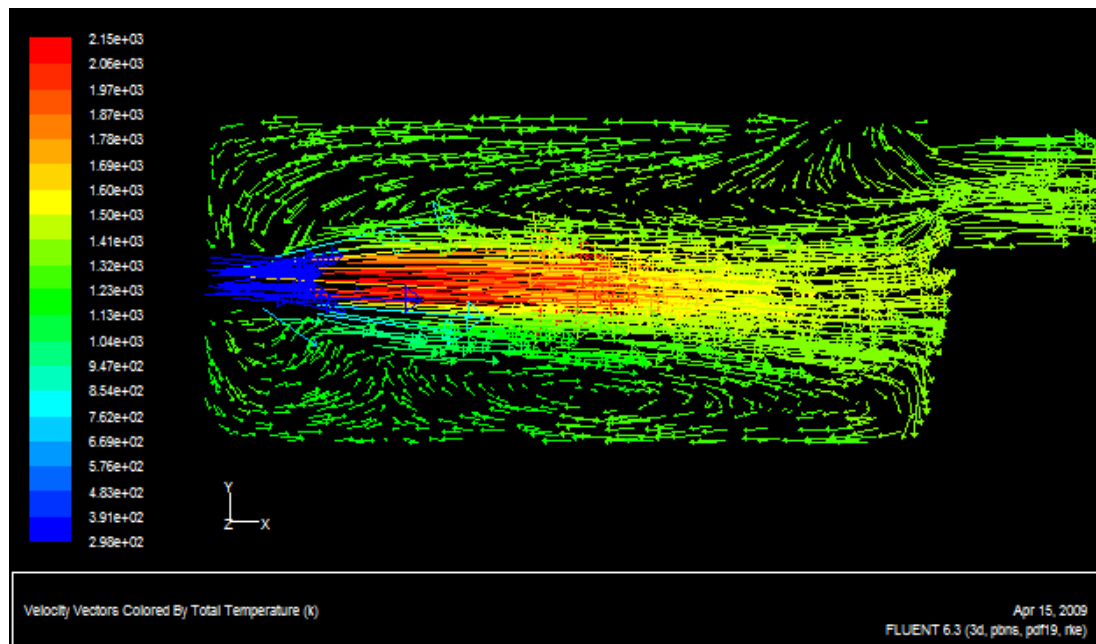


Figure 4.3: Velocity vector based on total temperature of the furnace.

4.4 Comparison between simulation and experimental result

Table 4.2 shows the comparison of flue temperature between simulation and experimental data. As it shown, the simulation results clearly follow the experimental data trend which is slowly decreases with increasing excess air ratio. The simulation was not included thermal NO model and N₂O route model because the simulation only intended to verify the temperature parameter. This exception has led to by big errors in simulation when compared to the experimental data. The reason is when NO_x emission is present, the temperature will be decreases further compared to the simulation result which exclude the NO_x emission. Therefore, this developed simulation model have to be further improved in order to obtain high accuracy prediction of NO_x emissions and its effect on temperature distribution.

Table 4.2: Comparison of flue temperature.

Excess Air, λ	Measured Exhaust Temperature, K	Predicted Exhaust Temperature, K	Percent Error, %
1.248	1007	1305.5249	29
1.299	1003	1302.5225	29
1.362	1000	1204.0127	20
1.417	986	1195.4402	21

On the other hand, the flame temperature comparison as shown in table 4.3 shows a high accuracy simulation results when compared to the experimental data. The trend of the simulation results also follows the experimental data which is the temperature is gradually decreases with increasing excess air ratio. The simulation result for flame temperature was able to achieve high accuracy when compared to the simulation result for exhaust temperature because the flame was the initial part of the combustion process. When the oxygen and fuel reacted together with the presence of ignition source, there was little or no NO_x emission produced from the initial reaction. NO_x is produced is depended on temperature level which also associated with certain excess air ratio [2]. The NO_x emission is linearly increased with increasing amount of excess air ratio. Therefore, at the flame structure, the reaction was so fast, there is no space for formation of NO_x, only at surrounding the flame its was able to form because of turbulence distribution of the temperature [2].

Table 4.3: Comparison of flame temperature.

Excess Air, λ	Measured Flame Temperature, K	Predicted Flame Temperature, K	Percent Error, %
1.248	1437	1518.8181	5.6
1.299	1436	1515.1814	5.5
1.362	1442	1505.3542	4.4
1.417	1443	1493.9243	3.5

In order to further understand this result, the variation of the maximum furnace temperature was given in figure 4.3 as a function of excess air ratio. It can be seen that the peak temperature in the furnace rises as excess air ratio increases. In fact, when oxygen concentration in reaction zone increases as excess air ratio increases, it will result in higher flame temperature [2]. This however only applies to excess air ratio below 1.25 because after the excess air ratio has exceeded the air/fuel ratio, the combustion began to suffer heat loss as more heat are loss to the air that being supplied in excess. This can be seen in figure 4.1 where the flame length becomes shorter with increasing excess air. When excess air ratio is lower than 1.25, the peak temperature becomes higher than 2000 K. When excess air ratio reaches to 1.30 and above, the peak temperature decreases to below 2000 K. In the other hand, even with higher excess air ratio being supplied, the rate of temperature decrease does not drop suddenly as shown in Figure 4.4 as its gradually decrease.

Furthermore, Figure 4.1 also shows that the temperature distribution is very sensitive to excess air ratio and was distributed accordingly based on turbulence inside the furnace.

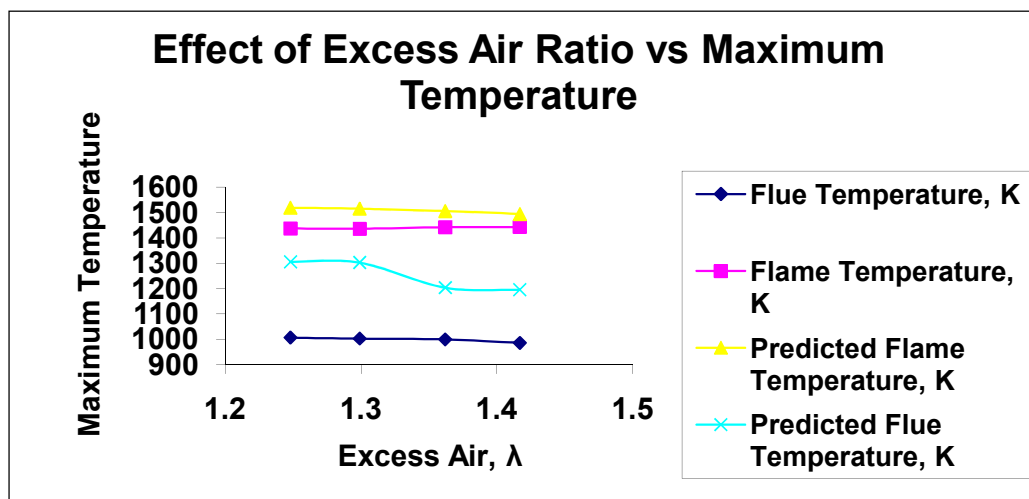


Figure 4.4: Effect of excess air ratio on flue temperature and flame temperature.

CHAPTER 5

CONCLUSION & RECOMMENDATIONS

From this project, it is important to know what going on inside today industrial furnace or combustion chamber. Without using CFD simulation programme, it is very difficult to know how temperature distribution or the NO_x or O₂ concentration inside the chamber or furnace. Moreover, it may be given very high cost or long operating hours in order to determine them through experiment. Hence, through simulation, we are able to reduce of that disadvantages and expecting the simulation result to converge with the experiment result within minimal error percentage in order to establish a developed model which provides a basis for further studies.

5.1 Conclusions

In this present work, CFD was used to simulate a combustion process inside a furnace with the objectives of observation of temperature distribution and heat transfer patterns based on excess air ratio parameter. The excess air ratio that was used is 1.248, 1.299, 1.362, and 1.417. From the experiment, the result shows that at increasing excess air ratio, the temperature of the flame and exhaust decrease gradually. The simulation was considered as a success because it was able to follow the trend that is set by the experimental result. The simulation results were able to achieve good agreement with the experimental result whereas with increasing excess air ratio, the temperature will decrease gradually. Moreover, the simulation was able to show what experimental data could not, which was the temperature distribution and turbulence flow inside the chamber. The flame of the process was shown

decreasing in length as the excess air ratio increases.

CFD simulation model has been developed to simulate combustion process inside pilot scale furnace and was able to come into good agreement with the experimental result. Moreover, CFD has the advantages of reduce cost, time and optimize design significantly.

5.2 Recommendations

To increase efficiency, need to supply high temperature air for combustion. Furthermore, suitable air/fuel ratio must be maintained for optimum operation, reduce NO_x emission. The use of CFD in designing and performance testing instead of real prototype and pilot testing. Lastly, the current simulation model that has been developed can be used to simulate full scale single flame furnace or boilers for NO_x emission and deposition effect.

REFERENCES

- [1] Aoki H, Suzuki A, Hisaeda Y, Suwa Y, Nakagawa T, Yaga M, et al. Recent research and development of combustion simulation. *Heat Transfer Asian Res* 2001; 30/7:581–612.
- [2] W. Yang, M. Mörtberg, W. Blasiak, Influence of flame location on flame properties and NO emissions in combustion with high temperature air, *Scand. J. Metallurgy* 34 (1) (2005) 7–15.
- [3] http://www.habmigern2003.info/2_combustion-efficiency.html, August 2008
- [4] http://en.wikipedia.org/wiki/Air_fuel_ratio, August 2008
- [5] H.K Versteeg and W. Malalasekera., *An introduction to computational fluid dynamics: The finite volume method*
- [6] <http://www.p-a-hilton.co.uk/C492.pdf>, August 2008
- [7] <http://www.methanol.org/pdf/FuelProperties.pdf>, August 2008
- [8] FLUENT 6.1 User's Guide Volume 2, Fluent In., August 2008
- [9] Weihong Yang and Wlodzimierz Blasiak, Mathematical modelling of NO emissions from high temperature air combustion with nitrous oxide mechanism, *Fuel Processing Technology*, 943 – 957, 86(2005)
- [10] Weihong Yang and Wlodzimierz Blasiak, Numerical simulation of properties of a LPG flame with high temperature air, *Int. J. Thermal Sce.*, 973 – 985
- [11] Nabil Rafidi and Wlodzimierz Blasiak, Heat transfer characteristics of HiTAC heating furnace using regenerative burners, *Applied Thermal Engineering*, 2027–2034, 26 (2006)
- [12] Brereton, C., “Combustion Performance,” In Avidan, A., Grace, J.R., Knowlton, T. (Eds.), Blackie Academic and Professional, London, U.K. (1997).
- [13] Ferziger JH, M Peric, 1996, *Computational Methods for Fluid Dynamics*, Springer-Verlag, Berlin.

- [14] G.K. Batchelor, Introduction to Fluid Dynamics, Cambridge University Press, 1967
- [15] C.K. Westbrook, F.L. Dryer, Simplified reaction mechanisms for the oxidation of hydrocarbon fuels in flames, *Combust. Sci. Tech.* 27 (1981) 31–42.
- [16] Permchart W, Kouprianov VI. Emission performance and combustion efficiency of a conical fluidized-bed combustor firing various biomass fuels. *Biores Technol* 2004; 92:83–91.
- [17] Gungor, A. and N. Eskin, “Two dimensional Coal Combustion Modelling of CFB,” *Int. J. Thermal Sci.*, 47, 157 (2008).
- [18] Arthur JA. Reactions between carbon and oxygen. *Trans Faraday Soc* 1951;47:164–71.
- [19] H.K Versteeg and W. Malalasekera., *An introduction to computational fluid dynamics: The finite volume method*
- [20] FKSA, Technical Unit,. *Combustion Gas Lab Unit Manual*,.(2007)
- [21] <http://www.bacharach-training.com/combustionzone/efficiencytypes1.htm>, August 2008
- [22] <http://www.bacharach-training.com/combustionzone/threets1.htm>, August 2008
- [23] http://en.wikipedia.org/wiki/Computational_fluid_dynamics, August 2008
- [24] <http://www.p-a-hilton.co.uk/English/Products/Combustion/combustion.html>, August 2008
- [25] Yang W. and Blasiak W., (2002), Heat transfer processes numerical modelling in HiTAC test furnace. Technical Report No 4, Contract: P11952 – 1, 2, Royal Institute of Technology, Energy and Furnace Technology, Stockholm, May 2002, ISRN KTH/MSE-02/17 ENERGY/TR.
- [26] W. Blasiak, W. Yang, N. Rafidi, Physical properties of a high temperature flame of air and LPG on a regenerative burner, *Combust Flame* 136 (4) (2004) 567–569.
- [27] S. Orsino, R. Weber, U. Bollettini, Numerical simulation of combustion of natural gas with high-temperature air, *Combust. Sci. Technol.* 168 (2002) 1–34.
- [28] Magnussen B. F., Hjertager B. H., *Proceeding of The Combustion Institute*, 16, 719 (1976)
- [29] Magnussen B. F., *Eccomas Thematic Conference on Computational*

Combustion, Lisbon, Portugal, June, (2005)

- [30] JANICKA, J., KOLBE, W., KOLLMANN, W J., “Closure of the transport equation for the PDF of turbulent scalar fields”, *Journal Non-Equilibrium Thermodynamics*, 4:47, 1978.
- [31] Pope, S.B. “Computationally Efficient Implementation of Combustion Chemistry using In Situ Adaptive Tabulation”, *Combustion Theory and Modelling*, Vol. 1, pp 41-63, 1997
- [32] Borman, G. L., and Ragland, K. W., 1998, *Combustion Engineering*, WCB McGraw-Hill, New York, Chap. 6, pp. 216–221.
- [33] P. A. Libby and F. A. Williams (eds.), *Turbulent Reacting Flows*, Academic, New York, 1994. 3. Pope, S. B., “Computations of Turbulent Combustion: Progress and Challenges,” in *Twenty-Third Symposium (International) on Combustion*, The Combustion Institute, Pittsburgh, 1990, p. 591.
- [34] Nau, M., Wolfert, A., Maas, U., and Warnatz, J., “Applications of a Combined PDF/Finite Volume Scheme on Turbulent Methane Diffusion Flames,” in *Proc. 8th International Symposium on Transport Phenomena in Combustion*, San Francisco, 1995
- [35] <http://www.fluent.com/about/cfdhistory.htm>, August 2008

APPENDIX A: CFD COMPUTATIONAL TOOLS

To run a simulation, three main elements are needed:

- **Pre-processor:** A pre-processor is used to define the geometry for the computational domain of interest and generate the mesh of control volumes (for calculations). Generally, the finer the mesh in the areas of large changes, the more accurate the solution. Fineness of the grid also determines the computer hardware and calculation time needed. The pre-processor used for this project is called GAMBIT.
- **Solver:** The solver makes the calculations using a numerical solution technique, which can use finite difference, finite element, or spectral methods. Most CFD codes use finite volumes, which is a special finite difference method. First the fluid flow equations are integrated over the control volumes (resulting in the exact conservation of relevant properties for each finite volume), then these integral equations are discretised (producing algebraic equations through converting of the integral fluid flow equations), and finally an iterative method is used to solve the algebraic equations. (The finite volume method and discretisation techniques are described more in the next sections. CFD FLUENT code is used for solving the simulations in this project.
- **Post-Processor:** The post-processor provides for visualisation of the results, and includes the capability to display the geometry/mesh, create vector, contour, and 2D and 3D surface plots. Particles can be tracked throughout a simulation, and the model can be manipulated (i.e. changed by scaling, rotating, etc.), and all in full colour animated graphics. FLUENT also is the post-processor used for this project.

APPENDIX A1: CFD GOVERNING EQUATION

Continuity and Momentum Equations

For all flows, FLUENT solves conservation equations for mass and momentum. For flows involving heat transfer or compressibility, an additional equation for energy conservation is solved. For flows involving species mixing or reactions, a species conservation equation is solved or, if the non-premixed combustion model is used, conservation equations for the mixture fraction and its variance are solved. Additional transport equations are also solved when the flow is turbulent.

In this section, the conservation equations for laminar flow in an inertial (non-accelerating) reference frame are presented. The conservation equations relevant to heat transfer, turbulence modelling, and species transport will be discussed in the chapters where those models are described.

The Mass Conservation Equation

The equation for conservation of mass, or continuity equation, can be written as follows:

$$\frac{\partial \rho}{\partial t} + \nabla \cdot (\rho \vec{v}) = S_m$$

Equation A.1.1

Equation A.1.1 is the general form of the mass conservation equation and is valid for incompressible as well as compressible flows. The source S_m is the mass added to the continuous phase from the dispersed second phase (e.g., due to vaporization of liquid droplets) and any user-defined sources.

For 2D axisymmetric geometries, the continuity equation is given by:

$$\frac{\partial \rho}{\partial t} + \frac{\partial}{\partial x}(\rho v_x) + \frac{\partial}{\partial r}(\rho v_r) + \frac{\rho v_r}{r} = S_m$$

Equation A.1.2

where x is the axial coordinate, r is the radial coordinate, v_x is the axial velocity, and v_r is the radial velocity.

Momentum Conservation Equations

Conservation of momentum in an inertial (non-accelerating) reference frame is described by:

$$\frac{\partial}{\partial t}(\rho \vec{v}) + \nabla \cdot (\rho \vec{v} \vec{v}) = -\nabla p + \nabla \cdot (\overline{\overline{\tau}}) + \rho \vec{g} + \vec{F}$$

Equation A.1.3

where p is the static pressure, $\overline{\overline{\tau}}$ is the stress tensor (described below), and $\rho \vec{g}$ and \vec{F} are the gravitational body force and external body forces (e.g., that arise from interaction with the dispersed phase), respectively. \vec{F} also contains other model-dependent source terms such as porous-media and user-defined sources.

The stress tensor $\overline{\overline{\tau}}$ is given by:

$$\overline{\overline{\tau}} = \mu \left[(\nabla \vec{v} + \nabla \vec{v}^T) - \frac{2}{3} \nabla \cdot \vec{v} I \right]$$

Equation A.1.4

where μ is the molecular viscosity, I is the unit tensor, and the second term on the right-hand side is the effect of volume dilation.

For 2D axisymmetric geometries, the axial and radial momentum conservation equations are given by:

$$\begin{aligned} \frac{\partial}{\partial t}(\rho v_x) + \frac{1}{r} \frac{\partial}{\partial x}(r \rho v_x v_x) + \frac{1}{r} \frac{\partial}{\partial r}(r \rho v_r v_x) = \\ -\frac{\partial p}{\partial x} + \frac{1}{r} \frac{\partial}{\partial x} \left[r \mu \left(2 \frac{\partial v_x}{\partial x} - \frac{2}{3} (\nabla \cdot \vec{v}) \right) \right] + \frac{1}{r} \frac{\partial}{\partial r} \left[r \mu \left(\frac{\partial v_x}{\partial r} + \frac{\partial v_r}{\partial x} \right) \right] + F_x \end{aligned}$$

Equation A.1.5

And:

$$\begin{aligned} \frac{\partial}{\partial t}(\rho v_r) + \frac{1}{r} \frac{\partial}{\partial x}(r \rho v_x v_r) + \frac{1}{r} \frac{\partial}{\partial r}(r \rho v_r v_r) = -\frac{\partial p}{\partial r} + \frac{1}{r} \frac{\partial}{\partial x} \left[r \mu \left(\frac{\partial v_r}{\partial x} + \frac{\partial v_x}{\partial r} \right) \right] \\ + \frac{1}{r} \frac{\partial}{\partial r} \left[r \mu \left(2 \frac{\partial v_r}{\partial r} - \frac{2}{3} (\nabla \cdot \vec{v}) \right) \right] - 2 \mu \frac{v_r}{r^2} + \frac{2}{3} \frac{\mu}{r} (\nabla \cdot \vec{v}) + \rho \frac{v_z^2}{r} + F_r \end{aligned}$$

Equation A.1.6

Where:

$$\nabla \cdot \vec{v} = \frac{\partial v_x}{\partial x} + \frac{\partial v_r}{\partial r} + \frac{v_r}{r}$$

Equation A.1.7

and v_z is the swirl velocity.

Energy Conservation Equation

Conservation of energy is described by:

$$\frac{\partial}{\partial t}(\rho E) + \nabla \cdot (\vec{v}(\rho E + p)) = -\nabla \cdot \left(\sum_j h_j J_j \right) + S_h$$

Equation A.1.8**First Law of Thermodynamics**

“The energy change of rate in a fluid element equals the heat addition rate in the fluid element added with the rate of work done on the element.”

The energy equation for net energy (e) flow includes terms to account for energy flux from conduction, work done by surface forces (i.e. shear stress causing friction and heat loss – irreversible, or change in volume due to pressure), and finally a source term to account for chemical reactions or radiation (either an energy source or sink).

$$\frac{\partial(\rho e)}{\partial t} + \frac{\partial(\rho_j e)}{\partial x_j} = \frac{\partial q_j}{\partial x_j} - p \frac{\partial u_i}{\partial x_i} + \tau_{ij} \frac{\partial u_i}{\partial x_j} + \dot{S}$$

Equation A.1.9**Equation of state**

Fluids are nearly always in thermodynamic equilibrium. When two state

variables of a substance are known, an equation of state can be used to describe the other thermodynamic variables (these are pressure p , density ρ , specific internal energy i , and temperature T). The (simplified) perfect gas equation of state is:

$$p = \rho RT$$

Equation A.1.10

Density changes as a result of temperature (or pressure) variations in the flow field of compressible fluids. This equation links the mass conservation and momentum equations to the energy equation, making it possible to calculate temperature changes, for example, from changes in density when two of the state variables are known (i.e. density and pressure). In the case of incompressible fluids, the energy and mass/momentum equations cannot be linked, and the mass and momentum equations must be used to solve for the flow field, and it is not necessary to solve for the energy equation. In this project, the FLUENT solves for flow and temperature. The equation of state is used in the calculations to solve for the temperature field.

Newton's law of viscosity (empirical relation for viscosity μ)

$$\tau_{ij} = \mu \left(\frac{\partial u_i}{\partial x_j} + \frac{\partial u_j}{\partial x_i} \right) - \frac{2}{3} \mu \cdot \frac{\partial u_i}{\partial x_i} \cdot \delta_{ij}$$

Equation A.1.11

Equation A.1.11 can then be inserted into the momentum balance to solve for viscosity.

Fourier's second law of thermodynamics (empirical relation for thermal conductivity, k)

$$q_i = -k \frac{\partial T}{\partial x_i}$$

Equation A.1.12

Equation A.1.12 can then be inserted into the energy equation (Equation A.1.8) to solve for viscosity.

General Transport Equation

From the insertions into the momentum and energy balances, the general transport equation for property ϕ is:

$$\begin{matrix} \text{(I)} & \text{(II)} & \text{(III)} & \text{(IV)} \\ \frac{\partial(\rho\phi)}{\partial t} + \frac{\partial(\rho u_i \phi)}{\partial x_i} = \frac{\partial}{\partial x_i} \left[\Gamma_\phi \frac{\partial \phi}{\partial x_i} \right] + S_\phi \end{matrix}$$

Equation A.1.13

which also can be expressed as:

$$\frac{\partial(\rho\phi)}{\partial t} + \text{div}(\rho\phi\vec{u}) = \text{div}(\Gamma \text{grad}\phi) + S_\phi$$

Equation A.1.14

The first term **(I)** on the left side of Equation A.1.12 represents the rate of change of property ϕ in the control volume over time [accumulation]. The second term **(II)** on the left side is the convective term [convection], or the net rate of change in ϕ in the control volume due to flow of ϕ across the boundaries of the volume. The first term **(III)** on the right side represents a diffusive term where Γ is the diffusion coefficient (i.e. k or μ) [diffusion]. The final term **(IV)** is the source term

for the net rate of production of the property ϕ (i.e. in the case of heat-producing chemical reactions) inside the control volume [internal production source].

The general transport equation is the basis for the CFD finite volume calculations. The property of interest (i.e. u , v , w , or T) is inserted into the equation as ϕ , the appropriate diffusion coefficient selected for the variable Γ , and relevant source terms are included. Then each of the mass, momentum, and energy conservation equations are transformed into equations which can be used in the finite volume method to make the CFD computations. The equations are integrated over all the control volumes in the geometry of interest, taking the solution from one fluid element and using it as a start value for the next element. [Hjertager, 2007 & Versteeg and Malalasekera, 2007]

APPENDIX A.2: MODELLING TURBULENCE

Turbulent flows are characterized by fluctuating velocity fields. These fluctuations mix transported quantities such as momentum, energy, and species concentration, and cause the transported quantities to fluctuate as well. Since these fluctuations can be of small scale and high frequency, they are too computationally expensive to simulate directly in practical engineering calculations. Instead, the instantaneous (exact) governing equations can be time-averaged, ensemble-averaged, or otherwise manipulated to remove the small scales, resulting in a modified set of equations that are computationally less expensive to solve. However, the modified equations contain additional unknown variables, and turbulence models are needed to determine these variables in terms of known quantities.

FLUENT provides the following choices of turbulence models

1. Spalart-Allmaras model
2. k - ε models
 - a. Standard k - ε model
 - b. Renormalization-group (RNG) k - ε model
 - c. Realizable k - ε model
3. k - ω models
 - a. Standard k - ω model
 - b. Shear-stress transport (SST) k - ω model
4. v^2 - f model(add-on)
5. Reynolds stress model (RSM)
 - a. Linear pressure-strain RSM model

- b. Quadratic pressure-strain RSM model
 - c. Low-Re stress-omega RSM model
- 6. Detached eddy simulation (DES) model
 - a. Spalart-Allmaras RANS model
 - b. Realizable k- ϵ RANS model
 - c. SST k- ω RANS model
- 7. Large eddy simulation (LES) model
 - a. Smagorinsky-Lilly subgrid-scale model
 - b. WALE subgrid-scale model
 - c. Kinetic-energy transport subgrid-scale model

Reynold's Averaged Navier Stokes (RANS) Equations

This section describes the RANS equations, which form the basis for turbulence modelling.

Time-Averaged Properties

The variation in the velocity u in the x -direction as a function of time (transient flow) at a particular point in a fluid element in turbulent flow may be illustrated as in Figure A.1 below.

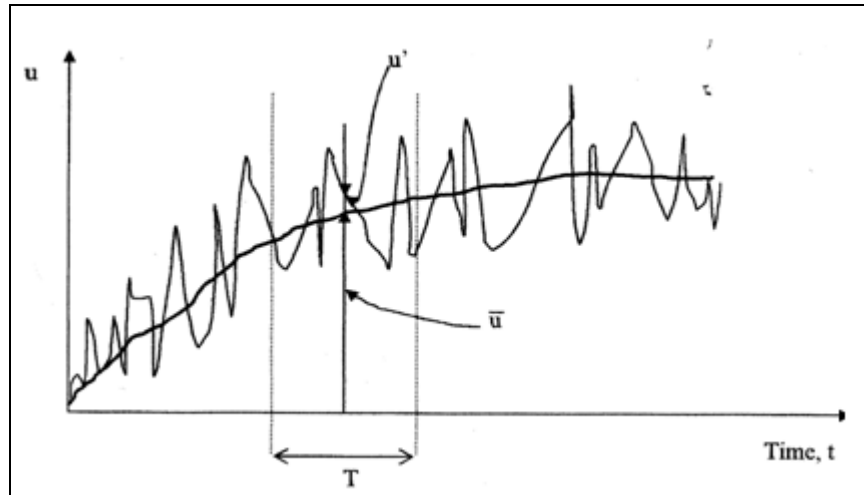


Figure A.1: Transient variations of velocity, u in turbulent flow. [Hjertager, 2005]

There are many small fluctuations occurring in turbulent flow. The fluctuations are due to vertical eddy motions which create strong mixing and a momentum exchange that causes acceleration of slower moving layers and deceleration of faster moving layers. Because of this momentum exchange, there are shear stresses, which are known as Reynolds stresses, from the turbulence. In addition to velocity fluctuations, concentration or heat fluxes can also occur over the fluid element faces.

Time-Averaged Navier-Stokes Equations

The Navier-Stokes equations for mass (Equation A.1.1) and momentum (Equations A.1.3-A.1.7) are expanded to include the time-averaged properties affected by the turbulence. As an example, the process for obtaining the time-averaged mass balance is described in some detail. The momentum balances and scalar transport equation follow a similar process (although more complicated), and the resulting time-averaged equation only is presented for these equations:

1. Time averaged mass balance

$$\frac{\partial \rho}{\partial t} + \frac{\partial(\rho u)}{\partial x} + \frac{\partial(\rho v)}{\partial y} + \frac{\partial(\rho w)}{\partial z} = 0$$

Equation A.2.1

2. Time averaged momentum equation

$$\begin{aligned} \frac{\partial}{\partial x}(\rho \bar{u^2}) + \frac{\partial}{\partial y}(\rho \bar{v} \cdot \bar{u}) + \frac{\partial}{\partial z}(\rho \bar{w} \cdot \bar{u}) = \\ -\frac{\partial \bar{p}}{\partial x} + \frac{\partial}{\partial x}(-\rho \bar{u'^2}) + \frac{\partial}{\partial y}(-\rho \bar{v' u'}) + \frac{\partial}{\partial z}(-\rho \bar{w' u'}) + \mu \cdot \left[\frac{\partial^2 \bar{u}}{\partial x^2} + \frac{\partial^2 \bar{u}}{\partial y^2} + \frac{\partial^2 \bar{u}}{\partial z^2} \right] \end{aligned}$$

Equation A.2.2

A process similar to that for the continuity equation above (replacing terms with time-averaged terms) is carried out for the momentum equations (Equations A.1.3-A.1.7). The resulting equation for the momentum equation in the x-direction is given as above: The equations for the other directions (y and z) are found using the same process, but not listed here. Density is assumed constant, and the new terms (*) appear as a result of the process of time averaging. The additional terms can be interpreted as extra turbulent stresses, known as the Reynolds stresses, to the mean velocity components (U, V, W), and are due to turbulent eddies causing fluctuating velocities and convective momentum.

3. Time averaged scalar transport equation

When deriving the time-averaged scalar transport equation (for scalar quantities like temperature), additional turbulent transport terms (*) also appear.

$$\frac{\partial(\rho \bar{\phi})}{\partial t} + \text{div}(\rho \bar{\phi} \bar{u}) = \text{div}(\Gamma_{\phi} \text{grad} \bar{\phi}) + \left[-\frac{\partial \bar{u' \phi'}}{\partial x} - \frac{\partial \bar{v' \phi'}}{\partial y} - \frac{\partial \bar{w' \phi'}}{\partial z} \right] + S_{\phi}^*$$

Equation A.2.3

The RANS equations for time-averaged mass, momentum and scalar transport equations have now been presented. They are used in this research project's turbulence models to calculate the flow properties.

Kinetic Energy

In order to make CFD calculations including effects of turbulence, the total turbulent kinetic energy k per unit mass at a particular point in a fluid element, and the turbulence intensity I , are determined for use in modelling of the turbulence. These are defined with the following expressions:

$$k = \frac{1}{2} (\overline{u'^2} + \overline{v'^2} + \overline{w'^2}) = \frac{1}{2} (\overline{u'_i \cdot u'_i})$$

Equation A.2.4

$$I = \frac{\left(\frac{2}{3} k \right)^{1/2}}{U_{ref}}$$

Equation A.2.5

For the *k-epsilon* and *k-omega* turbulence models used in this project, the velocity fluctuations are estimated and k calculated using Equation A.2.4. Turbulence intensity can then be found using the calculated k value and the reference mean flow velocity U_{ref} using Equation A.2.5. [Versteeg and Malalasekera, 2007 & Hjertager, 2005]

APPENDIX A3: MODELLING NON-PREMIX COMBUSTION

In non-premixed combustion, fuel and oxidizer enter the reaction zone in distinct streams. This is in contrast to premixed systems, in which reactants are mixed at the molecular level before burning. Examples of non-premixed combustion include pulverized coal furnaces, diesel internal-combustion engines and pool fires. Under certain assumptions, the thermo chemistry can be reduced to a single parameter: the mixture fraction. The mixture fraction, denoted by f , is the mass fraction that originated from the fuel stream. In other words, it is the local mass fraction of burnt and unburnt fuel stream elements (C, H, etc.) in all the species (CO_2 , H_2O , O_2 , etc.).

The approach is elegant because atomic elements are conserved in chemical reactions. In turn, the mixture fraction is a conserved scalar quantity, and therefore its governing transport equation does not have a source term. Combustion is simplified to a mixing problem, and the difficulties associated with closing non-linear mean reaction rates are avoided. Once mixed, the chemistry can be modelled as being in chemical equilibrium with the Equilibrium model, being near chemical equilibrium with the Steady Laminar Flamelet model, or significantly departing from chemical equilibrium with the Unsteady Laminar Flamelet model.

Non Premix Combustion and Mixture Fraction Theory

Non-premixed modelling involves the solution of transport equations for one or two conserved scalars (the mixture fractions). Equations for individual species are not solved. Instead, species concentrations are derived from the predicted mixture fraction fields. The thermochemistry calculations are pre-processed and then tabulated for look-up in FLUENT. Interaction of turbulence and chemistry is accounted for with an assumed-shape Probability Density Function (PDF).

Transport Equation for Mixture Fraction

Under the assumption of equal diffusivities, the species equations can be

reduced to a single equation for the mixture fraction, f . The reaction source terms in the species equations cancel, and thus f is a conserved quantity. While the assumption of equal diffusivities is problematic for laminar flows, it is generally acceptable for turbulent flows where turbulent convection overwhelms molecular diffusion. The Favre mean (density averaged) mixture fraction equation is:

$$\frac{\partial}{\partial t}(\rho \bar{f}) + \nabla \cdot (\rho \vec{v} \bar{f}) = \nabla \cdot \left(\frac{\mu_t}{\sigma_t} \nabla \bar{f} \right) + S_m + S_{\text{user}}$$

Equation A.3.1

The source term S_m is due solely to transfer of mass into the gas phase from liquid fuel droplets or reacting particles (e.g., coal). S_{user} is any user-defined source term. In addition to solving for the Favre mean mixture fraction, FLUENT solves a conservation equation for the mixture fraction variance, $\overline{f'^2}$:

$$\frac{\partial}{\partial t}(\rho \overline{f'^2}) + \nabla \cdot (\rho \vec{v} \overline{f'^2}) = \nabla \cdot \left(\frac{\mu_t}{\sigma_t} \nabla \overline{f'^2} \right) + C_g \mu_t (\nabla \bar{f})^2 - C_d \rho \frac{\epsilon}{k} \overline{f'^2} + S_{\text{user}}$$

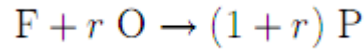
Equation A.3.2

where $f' = f - \bar{f}$. The default values for the constants σ_t , C_g , and C_d are 0.85, 2.86, and 2.0, respectively, and S_{user} is any user-defined source term. The mixture fraction variance is used in the closure model describing turbulence-chemistry interactions.

Mixture Fraction vs. Equivalence Ratio

The mixture fraction definition can be understood in relation to common measures of reacting systems. Consider a simple combustion system involving a fuel

stream (F), an oxidant stream (O), and a product stream (P) symbolically represented at stoichiometric conditions as:



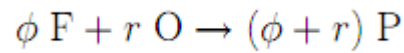
Equation A.3.3

where r is the air-to-fuel ratio on a mass basis. Denoting the equivalence ratio as ϕ , where:

$$\phi = \frac{(\text{fuel/air})_{\text{actual}}}{(\text{fuel/air})_{\text{stoichiometric}}}$$

Equation A.3.4

the reaction in Equation A.3.3, under more general mixture conditions, can then be written as:



Equation A.3.5

Looking at the left side of this equation, the mixture fraction for the system as a whole can then be deduced to be:

$$f = \frac{\phi}{\phi + r}$$

Equation A.3.6

Equation A.3.6 allows the computation of the mixture fraction at stoichiometric conditions ($\phi = 1$) or at fuel-rich conditions (e.g., $\phi > 1$), or fuel-lean conditions (e.g., $\phi < 1$).

APPENDIX B: FUEL PROPERTIES

Table B.1: Properties of Fuels

Property	Gasoline	No.2 Diesel Fuel	Methanol	Ethanol
Chemical Formula	C ₄ -C ₁₂	C ₃ -C ₂₃	CH ₃ OH	C ₂ H ₅ OH
Molecular Weight	100-105 ^(a)	≈200	32.04	46.07
Composition, Weight %				
Carbon	85-88 ^(b)	84-87	37.5	52.2
Hydrogen	12-15 ^(b)	33-16	12.6	13.1
Oxygen	0	0	49.9	34.7
Specific gravity, 60°F/60°F	0.72-0.78 ^(b)	0.81-0.89 ^(d)	0.796 ^(c)	0.796 ^(c)
Density, lb/gal@ 60°F	6.0-6.5 ^(b)	6.7-7.4 ^(d)	6.63 ^(b)	6.61 ^(b)
Boiling temperature, °F	80-437 ^(b)	370-650 ^(d)	149 ^(c)	172 ^(c)
Reid vapour pressure, psi	8-15 ^(k)	0.2	4.6 ^(o)	2.3 ^(o)
Octane no. ⁽¹⁾				
Research octane no.	90-100 ^(u)	--	107	108
Motor octane no.	81-90 ^(s)	--	92	92
(R+M)/2	86-94 ^(s)	N/A	100	100
Cetane no. ⁽¹⁾	5-20	40-55	--	--
Water solubility, @70°F				
Fuel in water, volume %	Negligible	Negligible	100 ^(c)	100 ^(b)
Water in fuel, volume %	Negligible	Negligible	100 ^(c)	100 ^(b)
Freezing point, °F	-40 ^(g)	-40-30 ⁽⁴⁾	-143.5	-173.2
Viscosity				
Centipoise @ 60°F	0.37-0.44 ^(3,p)	2.6-4.1	0.59 ⁽ⁱ⁾	1.19 ^(j)
Flash point, closed cup, °F	-45 ^(b)	165 ^(d)	52 ^(o)	55 ^(o)
Autoignition temperature, °F	495 ^(b)	≈600	867 ^(b)	793 ^(b)

Flammability limits, volume %				
Lower	1.4 ^(b)	1	7.3 ^(o)	4.3 ^(o)
Higher	7.6 ^(b)	6	36 ^(o)	19 ^(o)
Latent heat of vaporization				
Btu/gal @ 60°F	≈900 ^(b)	≈700	3,340 ^(b)	2,378 ^(b)
Btu/lb @ 60°F	≈150 ^(b)	≈100	506 ^(b)	396 ^(b)
Btu/lb air for stoichiometric mixture @ 60°F	≈10 ^(b)	≈8	78.4 ^(b)	44 ^(b)
Heating value(2)				
Higher (liquid fuel-liquid water) Btu/lb	18,800-20,400	19,200-20000	9,750 ⁽²⁾	12,800 ^(q)
Lower (liquid fuel-water vapour) Btu/lb	18,000-19,000	18,000-19,000	8,570 ^(b)	11,500 ^(q)
Higher (liquid fuel-liquid water) Btu/gal	124,800	138,700	64,250	84,100
Lower (liquid fuel-water vapour) Btu/gal @60°F	115,000	128,400	56,800 ⁽³⁾	76,000 ⁽³⁾
Heating value, stoichiometric mixture				
Mixture in vapour state, Btu/ft ³ @68°F	95.2 ^(b)	96.9 ^(5,q)	92.5 ^(b)	92.9 ^(b)
Fuel in liquid state, Btu/lb or air	1,290 ^(b)	--	1,330 ^(b)	1,280 ^(b)
Specific heat, Btu/lb °F	0.48 ^(g)	0.43	0.6 ^(j)	0.57 ^(j)
Stoichiometric air/fuel, weight	14.7 ⁽³⁾	14.7	6.45 ^(l)	9 ^(l)
Volume % fuel I vaporised stoichiometric mixture	2 ^(b)	--	12.3 ^(b)	6.5 ^(b)

Property	MTBE	Propane	Compressed Natural Gas (CNG)	Hydrogen
Chemical Formula	$(\text{CH}_3)_3\text{COCH}_3$	C_3H_8	CH_4	H_2
Molecular Weight	88.15	44.1	16.04	2.02 ^(x)
Composition, Weight %				
Carbon	66.1	82	75	0
Hydrogen	13.7	18	25	100
Oxygen	18.2	--	--	0
Specific gravity, 60°F/60°F	0.744 ^(m)	0.508	0.424	0.07 ^(u)
Density, lb/gal@ 60°F	6.19 ^(m)	4.22	1.07 ^(r)	--
Boiling temperature, °F	131 ^(c)	-44	-259	-4,230 ^(u)
Reid vapour pressure, psi	7.8 ^(e)	208	2,400	--
Octane no. ⁽¹⁾				
Research octane no.	116 ^(t)	112	--	130+
Motor octane no.	101 ^(t)	97	--	--
(R+M)/2	108 ^(t)	104	120+	--
Cetane no. ⁽¹⁾	--	--	--	--
Water solubility, @70°F				
Fuel in water, volume %	4.3 ^(e)	--	--	--
Water in fuel, volume %	1.4 ^(e)	--	--	--
Freezing point, °F	-164 ^(c)	-305.8	-296	-435 ^(v)
Viscosity				
Centipoise @ 60°F	0.35 ^(j)	--	--	
Flash point, closed cup, °F	-14 ^(e)	-100 to -150	-300	--
Autoignition temperature, °F	815 ^(e)	850-950	1,004	1,050-1,080

Flammability limits, volume %				
Lower	1.6 ^(e,k)	2.2	5.3	4.1 ^(u)
Higher	8.4 ^(e,k)	9.5	15	74 ^(u)
Latent heat of vaporization				
Btu/gal @ 60°F	863 ^(s)	775	--	--
Btu/lb @ 60°F	138 ^(s)	193.1	219	192.1 ^(v)
Btu/lb air for stoichiometric mixture @ 60°F	11.8	--	--	--
Heating value(2)				
Higher (liquid fuel-liquid water) Btu/lb	18,290 ^(h)	21,600	23,600	61,002 ^(v)
Lower (liquid fuel-water vapour) Btu/lb	15,100 ^(h)	19,800	21,300	51,532 ^(v)
Higher (liquid fuel-liquid water) Btu/gal	--	91,300	--	--
Lower (liquid fuel-water vapour) Btu/gal @60°F	93,500 ⁽⁴⁾	84,500	19,800 ⁽⁶⁾	--
Heating value, stoichiometric mixture				
Mixture in vapour state, Btu/ft ³ @68°F	--	--	--	--
Fuel in liquid state, Btu/lb or air	--	--	--	--
Specific heat, Btu/lb °F	0.5 ⁽ⁱ⁾	--	--	--
Stoichiometric air/fuel, weight	11.7 ⁽ⁱ⁾	15.7	17.2	34.3 ^(u)
Volume % fuel I vaporised stoichiometric mixture	2.7 ⁽ⁱ⁾	--	--	--

Notes:

- (1.) Octane values are for pure components. Laboratory engine Research and Motor octane rating procedures are not suitable for use with neat oxygenates. Octane values obtained by these methods are not useful in determining knock-limited compression ratios for vehicles operating on neat oxygenates and do not represent octane performance of oxygenates when blended with hydrocarbons. Similar problems exist for cetane rating procedures.
- (2.) The higher heating value is cited for completeness only. Since no vehicles in use, or currently being developed for future use, have power plants capable of condensing the moisture of combustion, the lower heating value should be used for practical comparisons between fuels.
- (3.) Calculated
- (4.) Pour Point, ASTM D 97 from Reference (c).
- (5.) Based on cetane.
- (6.) For compressed gas at 2,400 psi.

Sources:

- (a.) The basis of this table and associated references was taken from: American Petroleum Institute (API), Alcohols and Ethers, Publication No. 4261, 2nd ed. (Washington, DC, July 1988), Table B-1.
- (b.) "Alcohols: A Technical Assessment of Their Application as Motor Fuels," API Publication No. 4261, July 1976.
- (c.) Handbook of Chemistry and Physics, 62nd Edition, 1981, The Chemical Rubber Company Press, Inc.
- (d.) "Diesel Fuel Oils, 1987," Petroleum Product Surveys, National Institute for Petroleum and Energy Research, October 1987.
- (e.) ARCO Chemical Company, 1987.
- (f.) "MTBE, Evaluation as a High Octane Blending Component for Unleaded Gasoline," Johnson, R.T., Taniguchi, B.Y., Symposium on Octane in the 1980's, American Chemical Society, Miami Beach Meeting, September 10-15, 1979.

APPENDIX C: FLUENT SIMULATION RESULT

1. Excess Air Ratio = 1.248

Flow1

$T_{\text{flame}} = [1518.8181, 2128.2273]$ K

$T_{\text{flue}} = [1305.5249, 1396.9363]$ K

Max T= 2128.227 K

Volume average T=1276.288

Area average T= 1266.8604 K

Volume-Weighted Average

Total Temperature (k)

fluid	1276.2878
-------	-----------

Area-Weighted Average

Static Temperature (k)

default-interior	1276.3988
inlet_air	436.12888
inlet_fuel	303.76755
nozzle	301.53888
outlet_flue	1301.0883
plane-z	1328.4739
wall	1000.0071
Net	1266.8604

Total Heat Transfer Rate (w)

inlet_air	144.85741
inlet_fuel	-2188.075
nozzle	0
outlet_flue	8817.7031
wall	-6792.5586
Net	-18.073013

X direction of Allocating 40x40=1600 pixel map.

1276 pixels filled, area = 0.169882

Area of surfaces (0 2 1 4 3 6 5) projected onto plane (1, 0, 0): 0.16988165

Z direction of Allocating 101x40=4040 pixel map.

3575 pixels filled, area = 0.474375

Area of surfaces (0 2 1 4 3 6 5) projected onto plane (0, 0, 1): 0.47437498

Y direction of Allocating 40x101=4040 pixel map.

3562 pixels filled, area = 0.47265

Area of surfaces (0 2 1 4 3 6 5) projected onto plane (0, 1, 0): 0.47264998

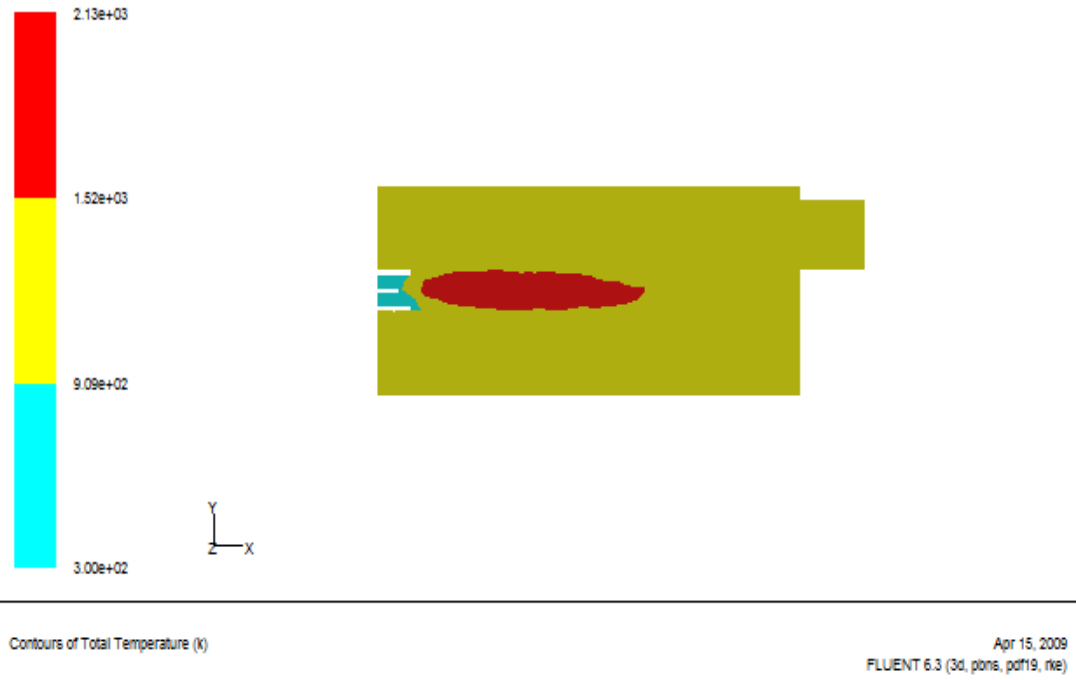


Figure C1: Contours of Flame Temperature Cross Section for $\lambda = 1.248$.

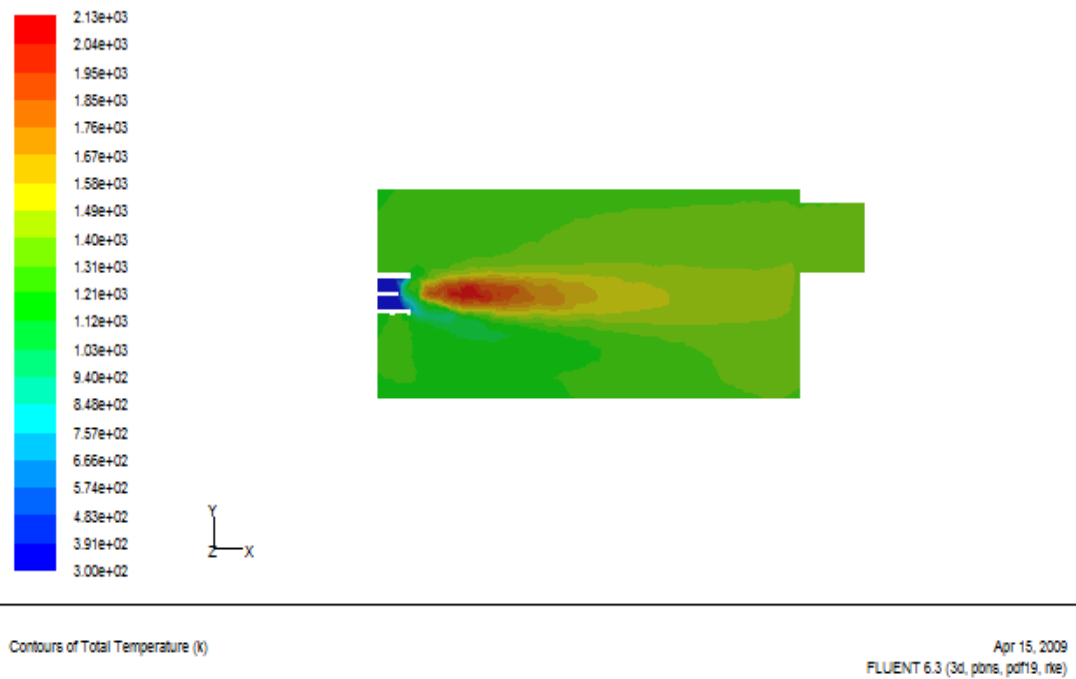


Figure C2: Contours of Total Temperature Distribution Cross Section for $\lambda = 1.248$.

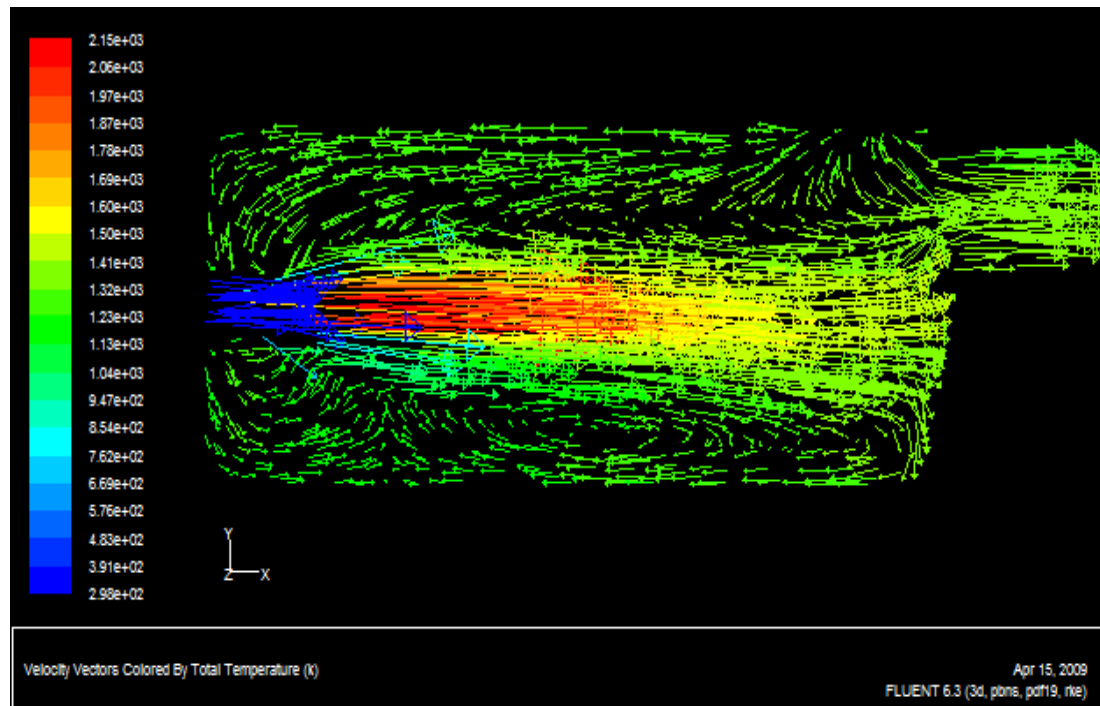


Figure C3: Velocity Vector of Temperature Distribution Cross Section for $\lambda = 1.248$.

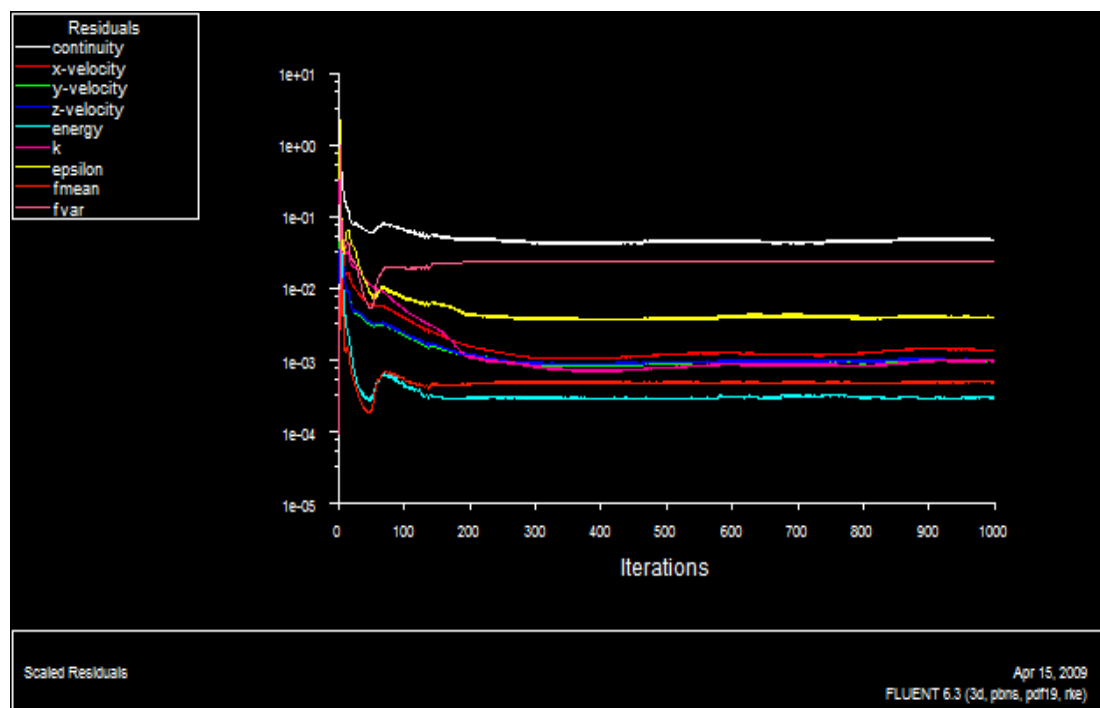


Figure C4: Residual Iteration for $\lambda = 1.248$.

2. Excess Air Ratio = 1.299

Flow 2

$T_{\text{flame}} = [1515.1814, 2122.7781]$ K

$T_{\text{flue}} = [1302.5225, 1393.662]$ K

Max T= 2128.227 K

Volume-Weighted Average

Total Temperature (k)

fluid	Total Temperature (k)
fluid	1269.2187

Area-Weighted Average

Total Temperature (k)

Surface	Total Temperature (k)
default-interior	1269.272
inlet_air	304.75223
inlet_fuel	427.82965
nozzle	309.55206
outlet_flue	1326.3831
plane-z	1314.4219
wall	1234.3567
Net	1268.3594

Total Heat Transfer Rate

(w)

Surface	Total Heat Transfer Rate (w)
inlet_air	149.23972
inlet_fuel	-2188.082
nozzle	0
outlet_flue	8652.4453
wall	-6547.3457
Net	66.257294

X direction of Allocating 40x40=1600 pixel map.

1276 pixels filled, area = 0.169882

Area of surfaces (0 2 1 4 3 6 5) projected onto plane (1, 0, 0): 0.16988165

Y direction of Allocating 40x101=4040 pixel map.

3562 pixels filled, area = 0.47265

Area of surfaces (0 2 1 4 3 6 5) projected onto plane (0, 1, 0): 0.47264998

Z direction of Allocating 101x40=4040 pixel map.

3575 pixels filled, area = 0.474375

Area of surfaces (0 2 1 4 3 6 5) projected onto plane (0, 0, 1): 0.47437498

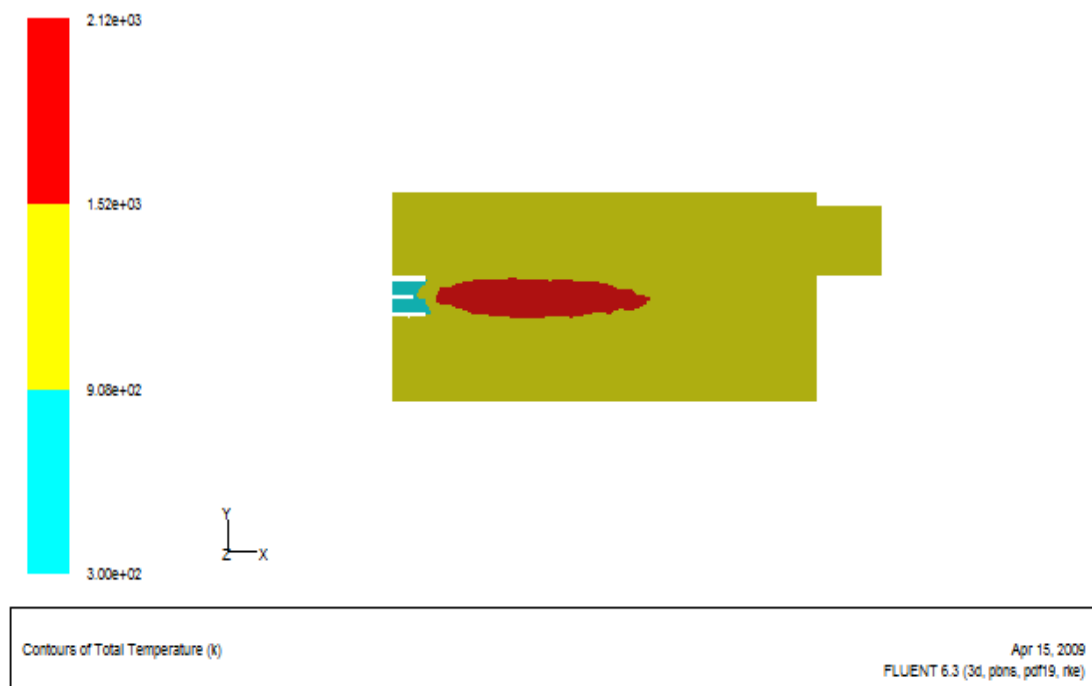


Figure C5: Contours of Flame Temperature Cross Section for $\lambda = 1.299$.

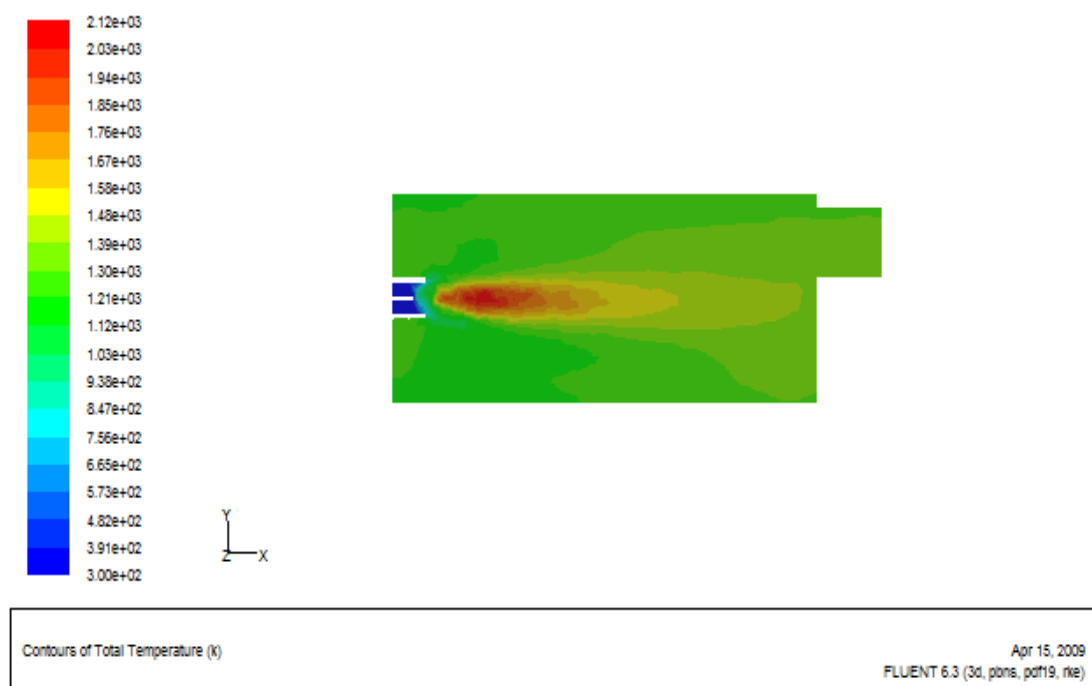


Figure C6: Contours of Temperature Distribution Cross Section for $\lambda = 1.299$.

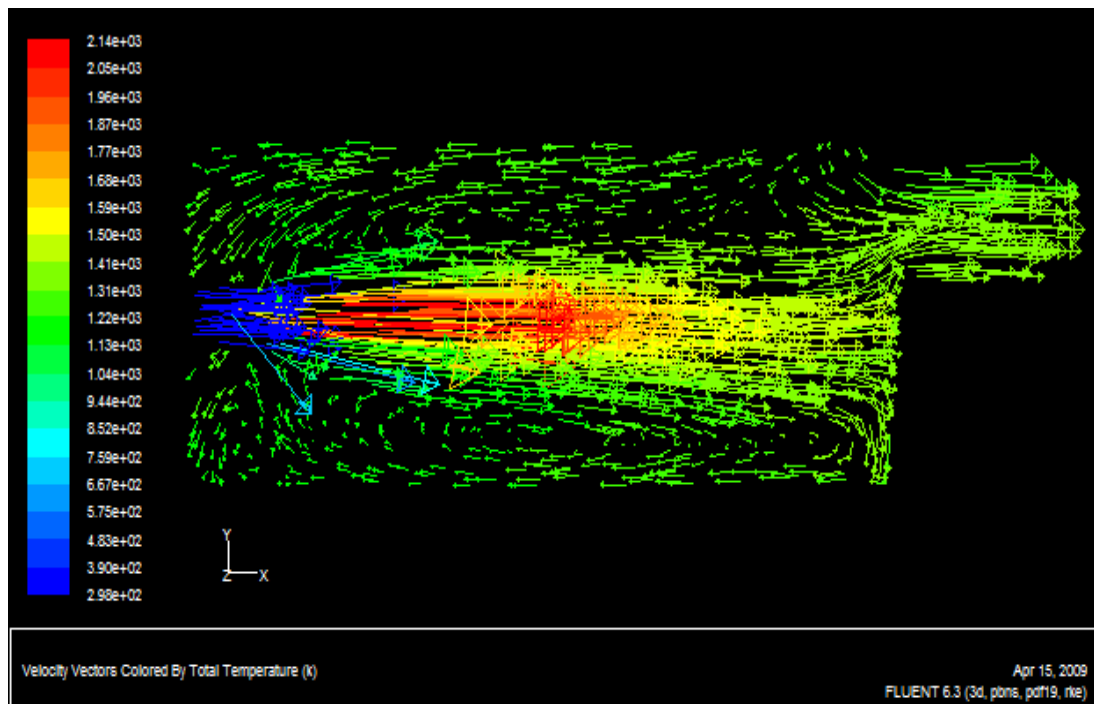


Figure C7: Velocity Vector of Temperature Distribution Cross Section for $\lambda = 1.299$.

3. Excess Air Ratio = 1.362

Flow 3

$T_{\text{flame}} = [1505.3542, 2108.0376]$ K

$T_{\text{flue}} = [1204.0127, 1294.4152]$ K

Max T = 2108.038 K

Area-Weighted Average Total Temperature (K)	
default-interior	1230.7167
inlet_air	304.73099
inlet_fuel	428.61514
nozzle	309.59683
outlet_flue	1282.879
plane-z	1275.5084
wall	1201.2572
Net	1229.9993

Volume-Weighted Average Total Temperature (k)	

fluid	1230.7099

Total Heat Transfer Rate (w)	

inlet_air	157.8593
inlet_fuel	-2167.0388
nozzle	0
outlet_flue	7896.5625
wall	-5991.0244

Net	-103.64143

X direction of Allocating 40x40=1600 pixel map.

1276 pixels filled, area = 0.169882

Area of surfaces (0 2 1 4 3 6 5) projected onto plane (1, 0, 0): 0.16988165

Y direction of Allocating 40x101=4040 pixel map.

3562 pixels filled, area = 0.47265

Area of surfaces (0 2 1 4 3 6 5) projected onto plane (0, 1, 0): 0.47264998

Z direction of Allocating 101x40=4040 pixel map.

3575 pixels filled, area = 0.474375

Area of surfaces (0 2 1 4 3 6 5) projected onto plane (0, 0, 1): 0.47437498

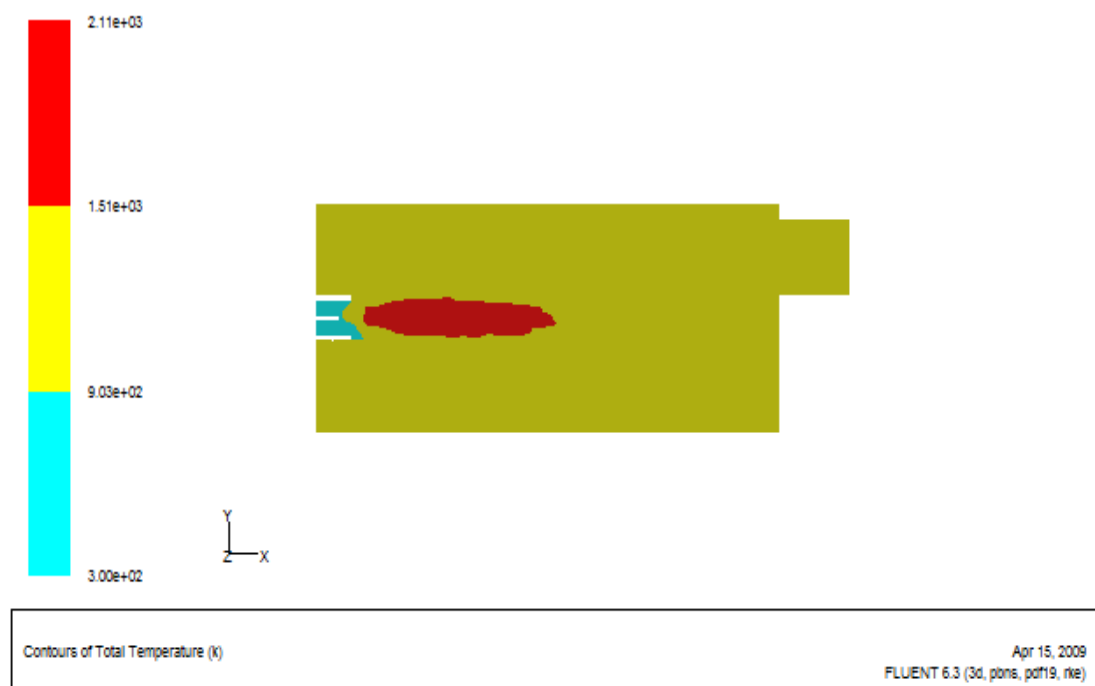


Figure C8: Contour of Flame Temperature Cross Section for $\lambda = 1.362$.

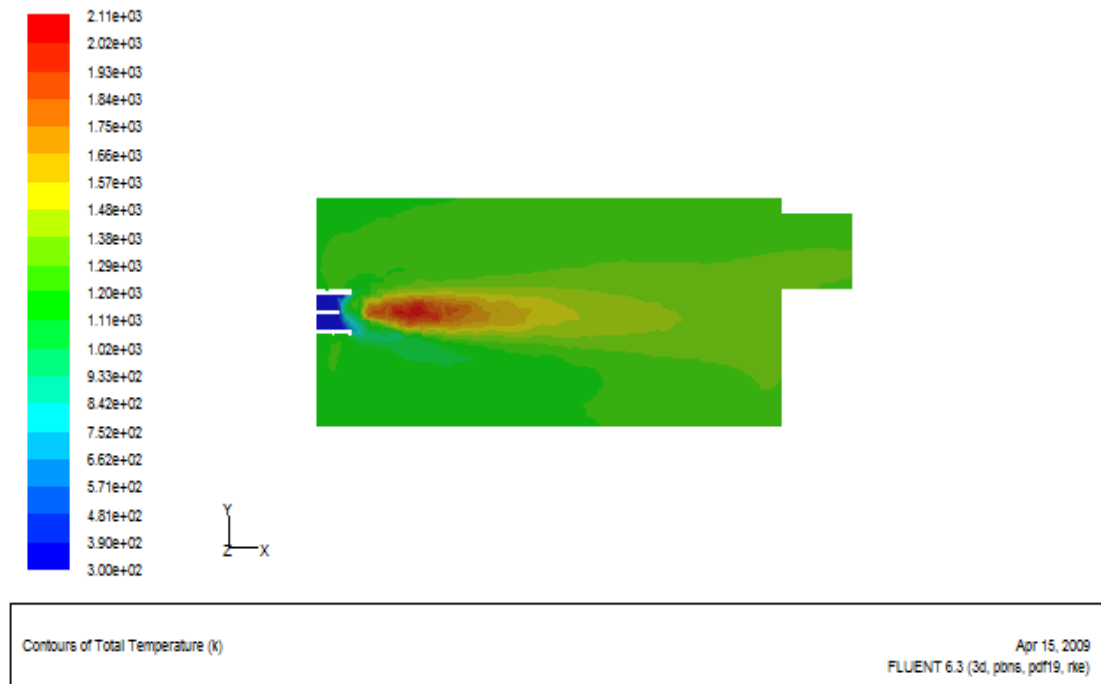


Figure C9: Contour of Temperature Distribution Cross Section for $\lambda = 1.362$.

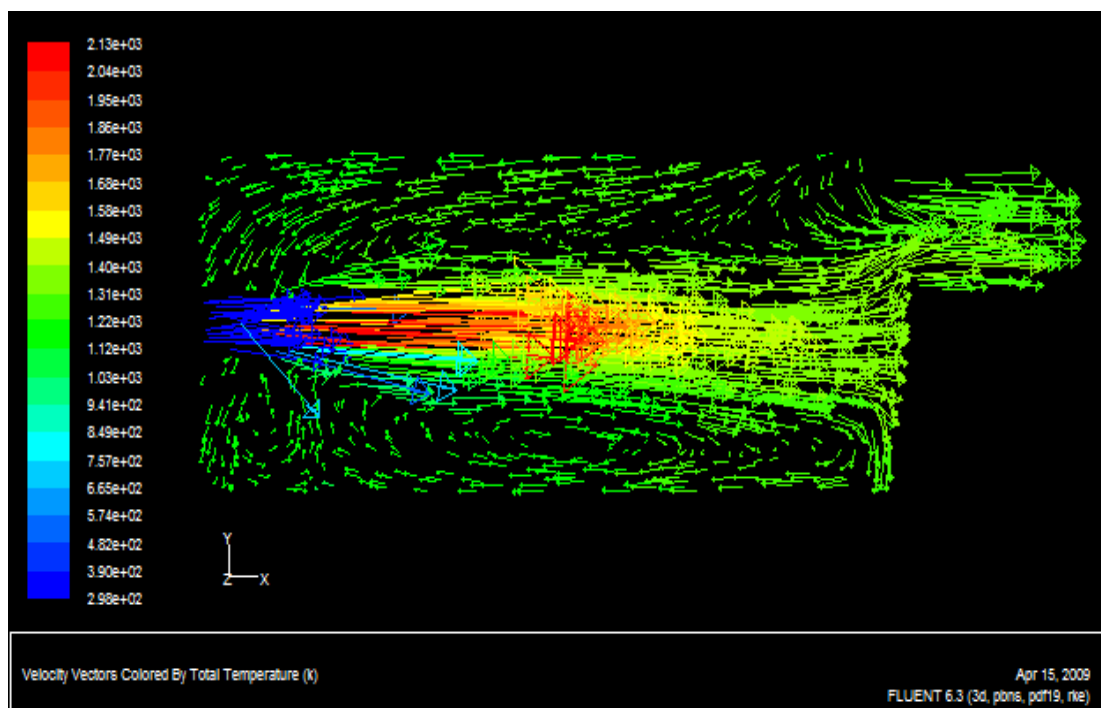


Figure C10: Velocity Vector of Temperature Distribution Cross Section for $\lambda = 1.362$.

4. Excess Air Ratio = 1.417

Flow 4

$T_{\text{flame}} = [1493.9243, 2090.8926]$ K

$T_{\text{flue}} = [1195.4402, 1284.9854]$ K

Max T= 2090.893 K

Area-Weighted Average

Total Temperature	(k)
default-interior	1213.1498
inlet_air	304.71307
inlet_fuel	430.09048
nozzle	309.6904
outlet_flue	1264.3656
plane-z	1257.6393
wall	1186.8171
Net	1212.5435

Volume-Weighted Average

Total Temperature	(k)
fluid	1213.2387

Total Heat Transfer Rate (w)

inlet_air	164.42247
inlet_fuel	-2167.0479
nozzle	0
outlet_flue	7582.0991
wall	-5483.9834
Net	95.490341

X direction of Allocating 40x40=1600 pixel map.

1276 pixels filled, area = 0.169882

Area of surfaces (0 2 1 4 3 6 5) projected onto plane (1, 0, 0): 0.16988165

Y direction of Allocating 40x101=4040 pixel map.

3562 pixels filled, area = 0.47265

Area of surfaces (0 2 1 4 3 6 5) projected onto plane (0, 1, 0): 0.47264998

Z direction of Allocating 101x40=4040 pixel map.

3575 pixels filled, area = 0.474375

Area of surfaces (0 2 1 4 3 6 5) projected onto plane (0, 0, 1): 0.47437498

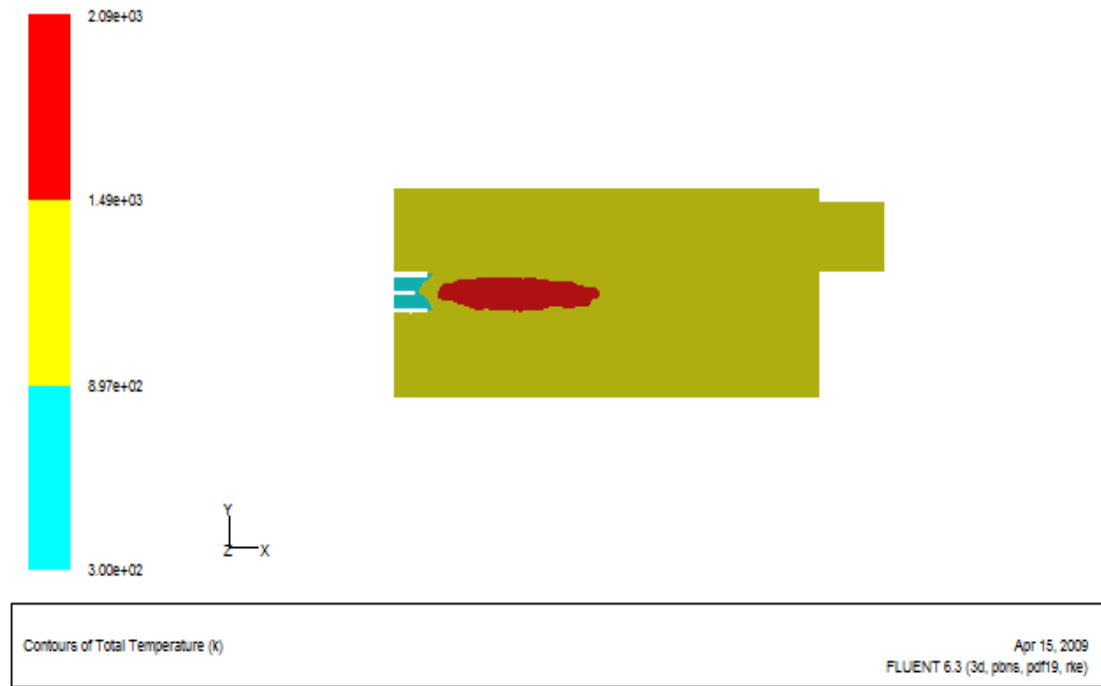


Figure C11: Contour of Flame Temperature Cross Section for $\lambda = 1.417$.

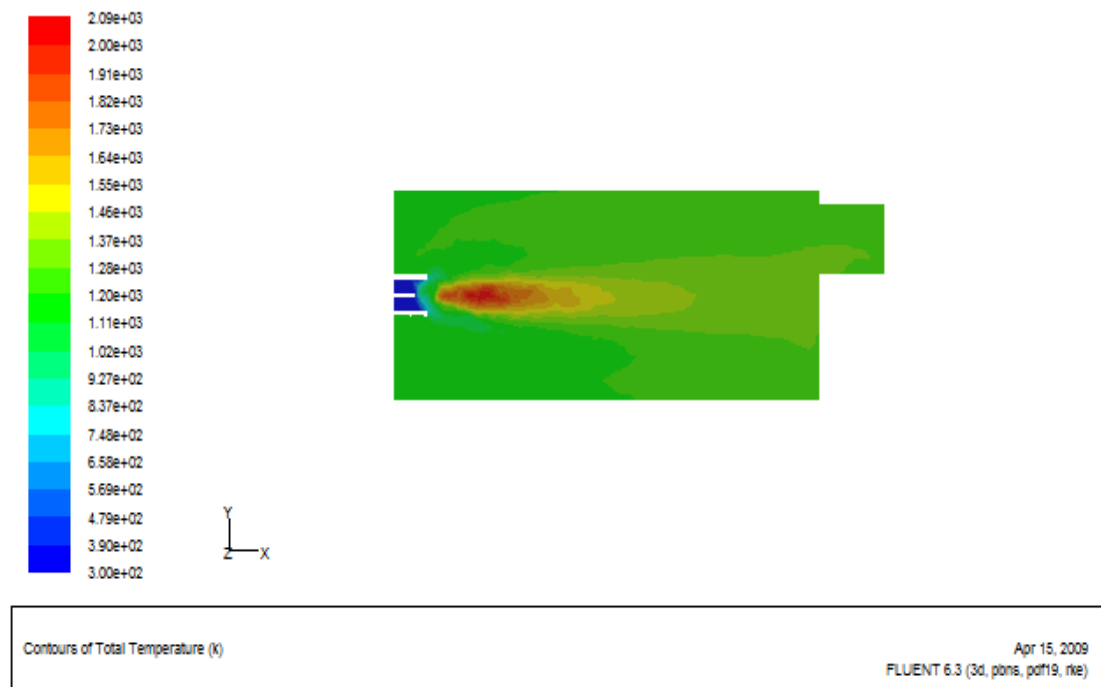


Figure C12: Contour of Temperature Distribution Cross Section for $\lambda = 1.417$.

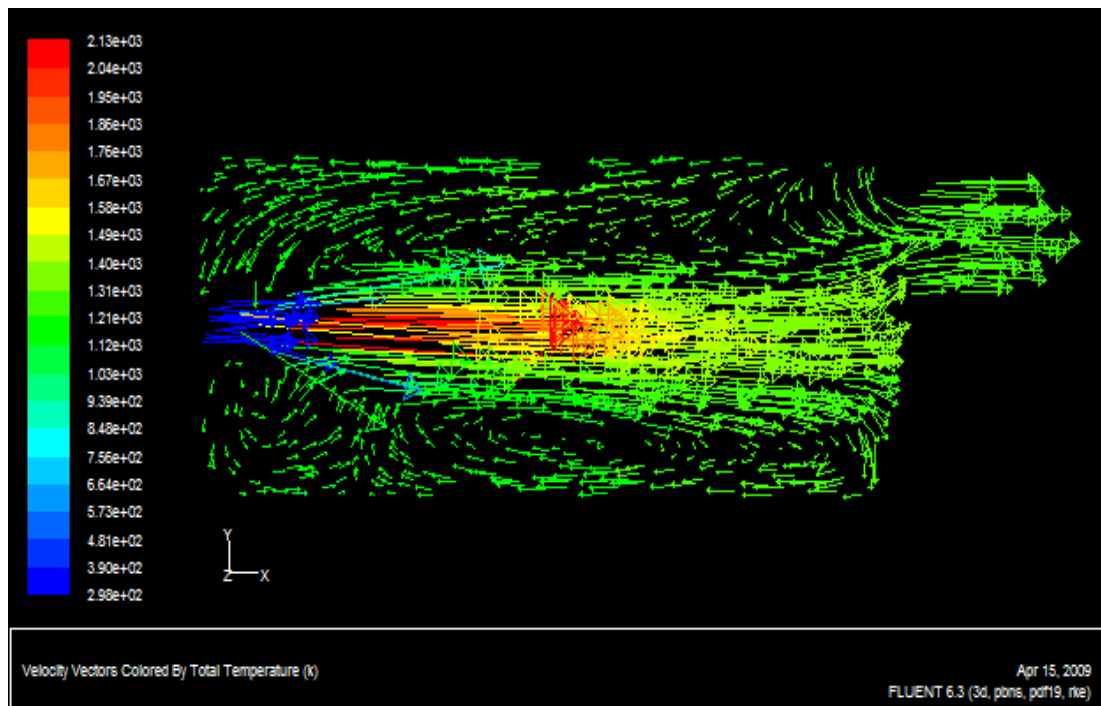


Figure C13: Velocity Vector of Temperature Distribution Cross Section for $\lambda = 1.417$.

APPENDIX D: EXPERIMENTAL RESULTS

C492- OBSERVATIONS

Date: August 2008 Fuel: Propane

Burner: STG146

Ambient Pressure: 1030 (mbar)
(C)

GAS

Stoichiometric A/F: 24 (by volume)

Density of Gas: 1.8 (kg/m³)

Stoichiometric A/F: 15.6 (by mass)

Ambient Temperature: 23

TEST NO.	1	2	3	4	5	6	7	8
Gas Pressure (cm H ₂ O)	7	7	7	7	7	7	7	7
Fan Damper Setting (No)	5	6	7	8	9	10	11	12
Gas Flow Rate Timer (sec)	116	119	122	123	124	124	119	120
Cooling Water Flowrate (g/s)	206	207	207	207	206	207	205	207
Cooling Water Inlet Temp. t ₁ (C)	15	15	15	15	15	15	15	15
Cooling Water Outlet Temp. t ₂ (C)	61	60	57	57	57	56	56	56
Air Inlet Temperature t ₃ (C)	22	22	21	21	21	21	22	22
Exhaust Temperature t ₄ (C)	776	755	734	730	727	713	724	717
O ₂ (%)	1.2	2.6	4.2	4.7	5.6	6.1	6.0	6.5
CO ₂ (%)	13.0	12.0	11.0	10.6	10.1	9.7	9.8	9.5
CO (ppm)	33	21	21	20	16	13	48	65
Excess Air (%)	5.7	14.6	24.8	29.9	36.2	41.7	40.3	45.2
Flame Temperature t ₅ (C)	1180	1174	1164	1163	1169	1170	1191	1198

Flame Length (cm)	70	70	68	68	65	65	60	60
Efficiency Nett (%)	71.4	69.7	68.0	67.2	65.8	65.1	64.8	64.1

C492- DERIVED RESULTS

**Date: August 2008 Fuel: Propane
Burner: STG146**

**Ambient Pressure: 1030 (mbar)
23 (C)**

GAS

Stoichiometric A/F: 24 (by volume) Density of Gas: 1.8 (kg/m³)

Stoichiometric A/F: 15.6 (by mass) Ambient Temperature:

TEST NO.	1	2	3	4	5	6	7	8
Gas Flow Rate (by Volume) (m ³ /Hr)	3.10	3.03	2.95	2.93	2.90	2.90	3.03	3.00
Air/Fuel Ratio (by Volume) (vol/vol)	25.37	27.50	29.95	31.18	32.69	34.01	33.67	34.75
Air Flow Rate (by Volume) (m ³ /Hr)	78.73	83.21	88.38	91.25	94.90	98.73	101.8 6	104.5 4
Gas Flow Rate (by mass) (kg/Hr)	5.59	5.45	5.31	5.27	5.23	5.23	5.45	5.40
A/F Ratio (by mass) (kg/kg)	16.49	17.88	19.47	20.26	21.25	22.11	21.89	22.65
Air Flow Rate (by mass) (kg/Hr)	92.11	97.35	103.4 1	106.76	111.03	115.52	119.1 8	122.3 2
Heat Input (Q _{in}) (kW)	77.59	75.63	73.77	73.17	72.58	72.58	75.63	75.00

Flue – Useful	a	(kW)	24.0						
Flue – Unburnt	b	(W)	2.19						
Flue – Vapor	c	(kW)	10.22						
Total Heat to Flue		(kW)	36.46						
d= (a+b+c)									
Heat to Water	e	(kW)	38.77						
Heat Output (Q_{out}) =(d+e)		(kW)	75.22						
Difference			0.54						
$(Q_{in} - Q_{out})/Q_{in}$		(%)							

Derived Result Sample Calculation

Gas Flow Rate (Volume)

$$\frac{360}{\text{Time(Sec)}} = \frac{360}{122} = 2.95 \text{ m}^3/\text{Hr}$$

Air Fuel Ratio (Volume)

Given Information

Stoichiometric A/F by volume = 24: 1

From analyzer, Excess Air (λ) = 49.7 %

$$\text{Stoichiometric} \times \left(\frac{\lambda}{100} + 1 \right) = 24 \times \left(\frac{24.8}{100} + 1 \right) = 29.95$$

Therefore, the ratio is **29.95:1**

Air Flow Rate (Volume)

=Gas Flow Rate x A/F_{vol}

=2.95 m³/hr x 29.95

=**88.35 m³/hr**

Gas Flow Rate (Mass)

=Volume Gas Flow Rate x Density of Fuel

=2.95 m³/hr x 1.8kg/m³

=**5.31 kg/hr**

Air Fuel Ratio (Mass)

Stoichiometric A/F by mass = 15.6:1

$$\text{Stoichiometric} \times \left(\frac{\lambda}{100} + 1 \right) = 15.6 \times \left(\frac{24.8}{100} + 1 \right) = 19.47$$

Therefore, the ratio is **19.47:1**

Air Flow Rate (Mass)

=Gas Flow Rate x A/F_{vol}

=5.31 kg/hr x 19.47

=**103.39 kg/hr**

Heat Input

=Mass Gas Flow Rate x Gross Calorific Value of Fuel

=5.31kg/hr x 50000 kJ/kg x 1hr/3600s

=73.75 kJ/s

=**73.75 kW**

USEFUL DATA PROVIDED BY HILTON COMBUSTION LABORATORY UNIT

Fuel	Stoichiometric A/F by Volume	Stoichiometric A/F by Mass	Theoretical Maximum CO₂ (%)	Gross Calorific Value (MJ/Kg)	Chemical Formula
Natural Gas	9.81 : 1	17.16 : 1	11.8	55.00	CH ₄
Propane	24 : 1	1.6 : 1	13.8	50.00	C ₃ H ₈
Butane	30 : 1	14.8 : 1	14.1	49.5	C ₄ H ₁₀
Kerosene	9.48 : 1	14.7 : 1	15.4	46.2	-
Gas Oil	9.82 : 1	14.4 : 1	15.4	45.5	-

LPG

Note that bottled gas generically referred as LPG (Liquefied Petroleum Gas) will be a blend of Propane and Butane in varying proportions that is obtained almost as a by-product of oil refining. The proportions of Propane and Butane will vary depending upon its source. In general however it will be acceptable to utilize the above characteristics for Propane when using LPG, as in almost cases Propane will be the main constituents of LPG.

Carbon Content of Liquid Fuels

For most light distillate fuels typical of those for use in the C492 unit the carbon content is 86%, the remainder being hydrogen (13%) and small amounts of sulphur depending on the fuel source.

Conversion Factor

10 mm H₂O = 1 cm H₂O = 1 mbar

1 ft³ = 0.02832 m³

1 Imperial gallon = 4.546 Litre

1 US gallon = 3.785 Litre

Typical Values of density (Kg/m³)

Item	Density
Kerosene	790
Gas Oil	835
Propane	1.85
Butane	2.45
Natural Gas	0.68

Molecular Weight of O₂ = 32

Molecular Weight of H₂ = 2

Molecular Weight of C = 12

Molecular Weight of N₂ = 28

Molecular Weight of H₂O = 18

Air = 79 % N₂, 21 % O₂ (by volume) or 76.7 % N₂, 23.3 % O₂ (by mass)